Supplementary Information

Simultaneous identification of viruses and viral variants with programmable DNA nanobait

Filip Bošković[1], Jinbo Zhu[1], Ran Tivony[1], Alexander Ohmann [1], Kaikai Chen[1], Mohammed F. Alawami[1], Milan Đorđević [1], Niklas Ermann[1], Joana Pereira Dias[2,3], Michael Fairhead[4], Mark Howarth[4], Stephen Baker[2,3], Ulrich F. Keyser[1,*]

[1] Cavendish Laboratory, University of Cambridge, JJ Thomson Avenue, Cambridge, CB3 0HE, UK

[2] University of Cambridge School of Clinical Medicine, Cambridge Biomedical Campus, Hills Road, Cambridge, CB2 0SP, UK

[3] Department of Medicine, University of Cambridge School of Clinical Medicine, Cambridge Biomedical Campus, Hills Road, Cambridge, CB2 0QQ, UK

[4] Department of Biochemistry, University of Oxford, South Parks Road, Oxford, OX1 3QU, UK

[*] *corresponding author*

This file includes:

Table of Contents

Section S1. DNA nanobait

Section S1.1 Nanobait design

Nanobait is assembled by mixing the linearized DNA scaffold (M13mp18, 7228 nt, Guild Biosciences, 100 nM) with short complementary oligos[1]. The basic set of oligos has 188 oligos which are 38 nt long and two terminal oligos that are 46 nt long (with four terminal T to avoid aggregation by blunt-end stacking[1–3]) that are complementary to the 7228 nt long scaffold. These oligos are provided in Table S2. Certain oligos from Table S2 were replaced with oligos that code references (listed in Table S3) and capture oligos that are specific for five targets. Nanobait has a detection region that is marked by two references and contains five capture strands specific to five targets (Figure S1a).

Each reference has six interspaced DNA dumbbells (schematic design is shown in Figure S1b) i.e. DNA double hairpins (5'-TCCTCTTTTGAGGAACAAGTTTTCTTGT-3') that are interpreted as one downward signal in nanopore events due to their close proximity[4,5]. In addition to the capturing oligo (which contains two regions, one comprising 38 nt complementary to the DNA scaffold and one comprising 20 nt complementary to the target), each capture site contains a partially complementary oligo (14 nt) that carries a label (Figure S1c). This single-stranded region of the capture strand contains a toehold (6 nt) needed for strand displacement reaction (SDR). Once a target is added to the solution, it first binds to the toehold and then it's able to displace the oligo with a label (Figure S1d). Hence, target presence is detected as the absence of oligo with a label (which is read as a missing peak in nanopore event).

Section S1.2 Linearization of circular single-stranded M13

Linearization of circular M13 scaffold (M13mp18, 7249 nt) is performed using double restriction digestion. Firstly, we bound an oligonucleotide (39 nt long, 5'-TCTAGAGGATCCCCGGGTACCGAGCTCGAATTCGTAATC-3') to the scaffold to create a double-stranded region for efficient enzyme digestion. Such a double-stranded region contains closely spaced restriction sites for EcoRI and BamHI enzymes. The double enzyme digestion is used to ensure complete linearization of the scaffold. We mixed 52 µL of scaffold (M13mp18, 100 nM) with 10 µL of 10 × CutSmart buffer (1 × buffer components are 50 mM potassium acetate, 20 mM Tris-acetate, 10 mM magnesium acetate, 100 µg/ml BSA, pH 7.9 at 25 °C; New England Biolabs), 2.5 µL of 39 nt long oligo (100 µM in H_20, IDT), and 33.5 µL of filtered Milli-Q water. The mix was heated to 65 °C for 30 s and slowly cooled down to 25 °C over ~40 min. After oligo

binding, 1 µL of EcoRI-HF enzyme (100,000 units/mL) and1 µL of BamHI-HF enzyme (100,000 units/mL) was added to the reaction and mixed by pipetting the full volume multiple times and incubated at 37 °C for 1 h. The cut scaffold was purified as previously described using NucleoSpin Gel and PCR Clean-up kit (Macherey-Nagel™)[1].

Section S1.3 Nanobait assembly

Nanobait is assembled by mixing the scaffold with a respective set of oligos. Briefly, we mixed 800 fmoles of the linearized scaffold with three times excess of oligos (2400 fmoles each) in 10 mM $MgCl_2$, 1 × Tris-HCl, pH 8.0. The reaction was heated to 70 °C for 30 s followed by linear cooling to 25 °C over 45 min. The excess oligos were removed with Amicon 0.5 mL filters with 100 kDa cut-off using a washing buffer (10 mM Tris-HCl, pH 8.0, 0.5 mM $MgCl_2$). The samples were centrifuged at 9,200 × g for 10 min twice, and after the filter was inverted, placed in a new tube, and spun down at 1,000 × g for 2 min. Nanobait concentration was estimated from a NanoDrop spectrophotometer or a Qubit fluorometer using Qubit™ dsDNA BR Assay Kit.

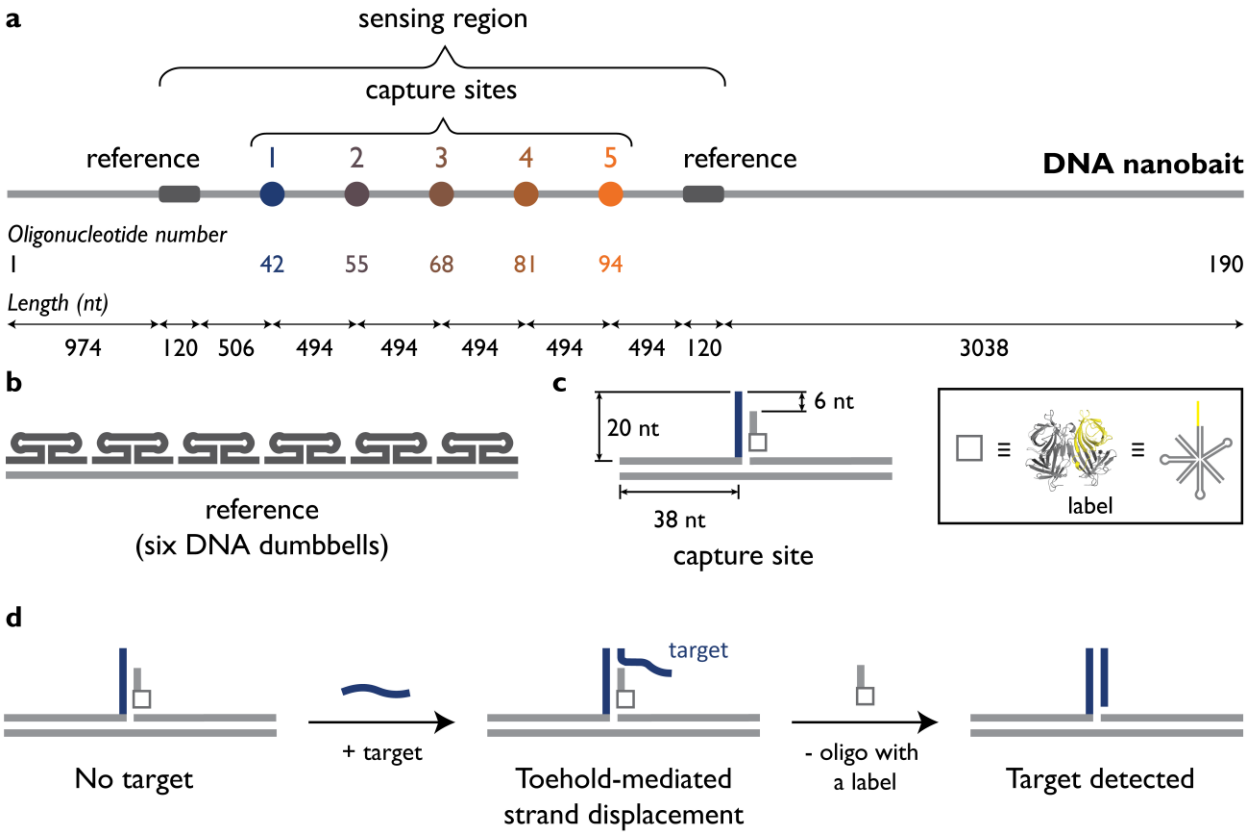

Figure S1. DNA nanobait schematic design. a) Nanobait contains a detection region that has two references (dark gray) and five capture sites for each target strand. Nanobait represents M13 DNA that is fully covered by oligonucleotides forming a double-stranded DNA with nicks. A standard set of 190

oligonucleotides was used and some of the oligonucleotides were replaced with a reference or capture strands. Oligo numbers replaced for each capture site is depicted below the nanobait. Lengths and distances between features on nanobait are represented as a number of nucleotides i.e. basepairs once a double-stranded molecule is formed. b) Reference contains six interspaced DNA dumbbells which are read as one downward signal in nanopore measurements. c) Capture site structure is represented by capture strand that has a 38 nt part complementary to the DNA scaffold and a 20 nt part that is fully complementary to a target strand. The oligo carrying the label is partially complementary to the capture strand (14 nt). The label can be either monovalent streptavidin or a DNA flower. d) The uncomplemented part of the capture strand (6 nt) is called the toehold and it serves as a seed for displacement (removal) of the oligo with a label by the target.

Section S2. Design of structural labels used for nanopore signal amplification

Specific identification of the presence or absence of the target sequence in solution is done by using nanopore sensing. In nanopore recordings, the "control" or absence of a target is detected as a downward signal or peak on a DNA event. This peak corresponds to a label that is attached to an oligonucleotide (oligo or strand) (further explained in Section S3). In this study, we demonstrated that both protein-based and DNA-based structures can be employed as labels.

As a protein-based label, we employed monovalent streptavidin (structure shown in Figure S2a) that has a single femtomolar affinity biotin binding site. Monovalent streptavidin expression and purification have been described previously[6]. Oligos have a biotin label on the 3' end via a C6 spacer arm (Integrated DNA Technologies) to which monovalent streptavidin binds.

As a DNA-based label, we assembled a DNA flower[7] that represents a 7-way junction as is illustrated in Figure S2b using four DNA strands as described in the next section. One of the strands (J4, Table S1) has 14 nt single-stranded part (in yellow) that is used as an anchor that binds to nanobait (further explained in Section S3).

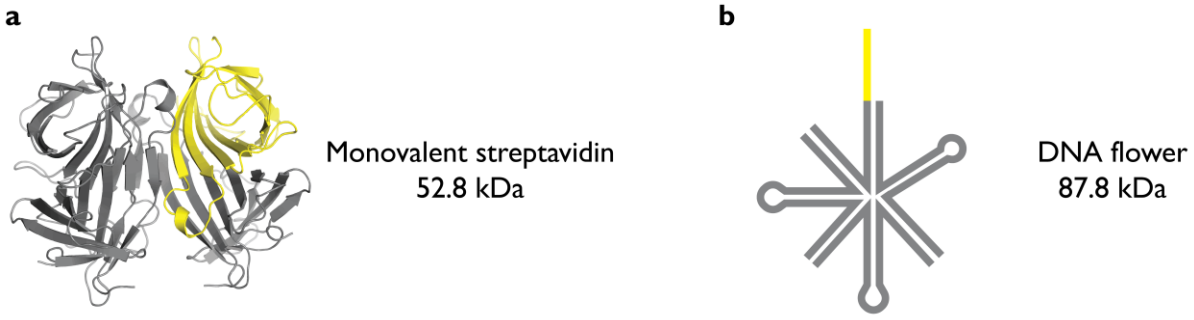

Figure S2. The designs of structures used in this study as labels. a) The tetramer is formed from one biotin-binding subunit in yellow and 3 non-binding subunits in gray (PDB ID: 5TO2). b) DNA flower represents a 7-way junction, designed with an arm length of 16 bp and loops with 4 T (gray). The region of oligo that binds to a respective site on the nanobait is in yellow.

Section S3. DNA flower synthesis

Three DNA flowers specific for each SARS-CoV-2 target (7-way junctions, 7WJa, 7WJb, and 7WJc) were prepared separately. Taking 7WJc as an example, 4 μM DNA strands J1, J2, J3,

and J4c (Table S1) were mixed in TM buffer (10 mM Tris-HCl, 10 mM $MgCl_2$, pH 8.0) and heated at 90 °C for 5 min, then cooled down to 65 °C for 15 min, 45 °C for 15 min, 37 °C for 20 min, 25 °C for 20 min and finally 4 °C for 20 min. Strand J4c was substituted by J4b to prepare 7WJb. For 7WJa, to avoid self-folding and improve the occupied fraction at site 43 on nanobait, J1, J2, J3 J4a, and C43 were mixed before annealing.

Supplementary Table S1. DNA flower oligonucleotides. The complementary parts are highlighted by using the same color.

Strand name	Sequence (5'→'3')
J1	GGATCAGAGCTGGACG ACAATGACGTAGGTCC TTTT GGACCTACGTCATTGT ACTATGGCACACATCC
J2	GCAAGACTCGTGCTCA CCGAATGCCACCACGC TTTT GCGTGGTGGCATTCGG CGTCCAGCTCTGATCC
J3	GGTTCAGCCGCAATCC TCGCCTGCACTCTACC TTTT GGTAGAGTGCAGGCGA TGAGCACGAGTCTTGC
J4a	TACTGCGCTTCGAT TT GGATGTGTGCCATAGT GGATTGCGGCTGAACC
J4b	AACTGAGGGAGCCT TT GGATGTGTGCCATAGT GGATTGCGGCTGAACC
J4c	AGACTAATTCTCCT TT GGATGTGTGCCATAGT GGATTGCGGCTGAACC

Supplementary Table S2. DNA scaffold complementary oligonucleotides

Oligo number	Sequence (5'→'3')
1	TTTTCGTAATCATGGTCATAGCTGTTTCCTGTGTGAAATTGTTATC
2	CGCTCACAATTCCACACAACATACGAGCCGGAAGCATA
3	AAGTGTAAAGCCTGGGGTGCCTAATGAGTGAGCTAACT
4	CACATTAATTGCGTTGCGCTCACTGCCCGCTTTCCAGT
5	CGGGAAACCTGTCGTGCCAGCTGCATTAATGAATCGGC
6	CAACGCGCGGGGAGAGGCGGTTTGCGTATTGGGCGCCA
7	GGGTGGTTTTTCTTTTCACCAGTGAGACGGGCAACAGC
8	TGATTGCCCTTCACCGCCTGGCCCTGAGAGAGTTGCAG
9	CAAGCGGTCCACGCTGGTTTGCCCCAGCAGGCGAAAAT
10	CCTGTTTGATGGTGGTTCCGAAATCGGCAAAATCCCTT
11	ATAAATCAAAAGAATAGCCCGAGATAGGGTTGAGTGTT
12	GTTCCAGTTTGGAACAAGAGTCCACTATTAAAGAACGT
13	GGACTCCAACGTCAAAGGGCGAAAAACCGTCTATCAGG
14	GCGATGGCCCACTACGTGAACCATCACCCAAATCAAGT
15	TTTTTGGGGTCGAGGTGCCGTAAAGCACTAAATCGGAA
16	CCCTAAAGGGAGCCCCCGATTTAGAGCTTGACGGGGAA
17	AGCCGGCGAACGTGGCGAGAAAGGAAGGGAAGAAAGCG
18	AAAGGAGCGGGCGCTAGGGCGCTGGCAAGTGTAGCGGT
19	CACGCTGCGCGTAACCACCACACCCGCCGCGCTTAATG
20	CGCCGCTACAGGGCGCGTACTATGGTTGCTTTGACGAG
21	CACGTATAACGTGCTTTCCTCGTTAGAATCAGAGCGGG
22	AGCTAAACAGGAGGCCGATTAAAGGGATTTTAGACAGG
23	AACGGTACGCCAGAATCCTGAGAAGTGTTTTTATAATC
24	AGTGAGGCCACCGAGTAAAAGAGTCTGTCCATCACGCA
25	AATTAACCGTTGTAGCAATACTTCTTTGATTAGTAATA
26	ACATCACTTGCCTGAGTAGAAGAACTCAAACTATCGGC
27	CTTGCTGGTAATATCCAGAACAATATTACCGCCAGCCA
28	TTGCAACAGGAAAAACGCTCATGGAAATACCTACATTT
29	TGACGCTCAATCGTCTGAAATGGATTATTTACATTGGC
30	AGATTCACCAGTCACACGACCAGTAATAAAAGGGACAT
31	TCTGGCCAACAGAGATAGAACCCTTCTGACCTGAAAGC
32	GTAAGAATACGTGGCACAGACAATATTTTTGAATGGCT
33	ATTAGTCTTTAATGCGCGAACTGATAGCCCTAAAACAT
34	CGCCATTAAAAATACCGAACGAACCACCAGCAGAAGAT
35	AAAACAGAGGTGAGGCGGTCAGTATTAACACCGCCTGC
36	AACAGTGCCACGCTGAGAGCCAGCAGCAAATGAAAAAT
37	CTAAAGCATCACCTTGCTGAACCTCAAATATCAAACCC
38	TCAATCAATATCTGGTCAGTTGGCAAATCAACAGTTGA
39	AAGGAATTGAGGAAGGTTATCTAAAATATCTTTAGGAG
40	CACTAACAACTAATAGATTAGAGCCGTCAATAGATAAT
41	ACATTTGAGGATTTAGAAGTATTAGACTTTACAAACAA
42	TTCGACAACTCGTATTAAATCCTTTGCCCGAACGTTAT
43	TAATTTTAAAAGTTTGAGTAACATTATCATTTTGCGGA

44	ACAAAGAAACCACCAGAAGGAGCGGAATTATCATCATA
45	TTCCTGATTATCAGATGATGGCAATTCATCAATATAAT
46	CCTGATTGTTTGGATTATACTTCTGAATAATGGAAGGG
47	TTAGAACCTACCATATCAAAATTATTTGCACGTAAAAC
48	AGAAATAAAGAAATTGCGTAGATTTTCAGGTTTAACGT
49	CAGATGAATATACAGTAACAGTACCTTTTACATCGGGA
50	GAAACAATAACGGATTCGCCTGATTGCTTTGAATACCA
51	AGTTACAAAATCGCGCAGAGGCGAATTATTCATTTCAA
52	TTACCTGAGCAAAAGAAGATGATGAAACAAACATCAAG
53	AAAACAAAATTAATTACATTTAACAATTTCATTTGAAT
54	TACCTTTTTTAATGGAAACAGTACATAAATCAATATAT
55	GTGAGTGAATAACCTTGCTTCTGTAAATCGTCGCTATT
56	AATTAATTTTCCCTTAGAATCCTTGAAAACATAGCGAT
57	AGCTTAGATTAAGACGCTGAGAAGAGTCAATAGTGAAT
58	TTATCAAAATCATAGGTCTGAGAGACTACCTTTTTAAC
59	CTCCGGCTTAGGTTGGGTTATATAACTATATGTAAATG
60	CTGATGCAAATCCAATCGCAAGACAAAGAACGCGAGAA
61	AACTTTTTCAAATATATTTTAGTTAATTTCATCTTCTG
62	ACCTAAATTTAATGGTTTGAAATACCGACCGTGTGATA
63	AATAAGGCGTTAAATAAGAATAAACACCGGAATCATAA
64	TTACTAGAAAAAGCCTGTTTAGTATCATATGCGTTATA
65	CAAATTCTTACCAGTATAAAGCCAACGCTCAACAGTAG
66	GGCTTAATTGAGAATCGCCATATTTAACAACGCCAACA
67	TGTAATTTAGGCAGAGGCATTTTCGAGCCAGTAATAAG
68	AGAATATAAAGTACCGACAAAAGGTAAAGTAATTCTGT
69	CCAGACGACGACAATAAACAACATGTTCAGCTAATGCA
70	GAACGCGCCTGTTTATCAACAATAGATAAGTCCTGAAC
71	AAGAAAAATAATATCCCATCCTAATTTACGAGCATGTA
72	GAAACCAATCAATAATCGGCTGTCTTTCCTTATCATTC
73	CAAGAACGGGTATTAAACCAAGTACCGCACTCATCGAG
74	AACAAGCAAGCCGTTTTTATTTTCATCGTAGGAATCAT
75	TACCGCGCCCAATAGCAAGCAAATCAGATATAGAAGGC
76	TTATCCGGTATTCTAAGAACGCGAGGCGTTTTAGCGAA
77	CCTCCCGACTTGCGGGAGGTTTTGAAGCCTTAAATCAA
78	GATTAGTTGCTATTTTGCACCCAGCTACAATTTTATCC
79	TGAATCTTACCAACGCTAACGAGCGTCTTTCCAGAGCC
80	TAATTTGCCAGTTACAAAATAAACAGCCATATTATTTA
81	TCCCAATCCAAATAAGAAACGATTTTTTGTTTAACGTC
82	AAAAATGAAAATAGCAGCCTTTACAGAGAGAATAACAT
83	AAAAACAGGGAAGCGCATTAGACGGGAGAATTAACTGA
84	ACACCCTGAACAAAGTCAGAGGGTAATTGAGCGCTAAT
85	ATCAGAGAGATAACCCACAAGAATTGAGTTAAGCCCAA
86	TAATAAGAGCAAGAAACAATGAAATAGCAATAGCTATC
87	TTACCGAAGCCCTTTTTAAGAAAAGTAAGCAGATAGCC
88	GAACAAAGTTACCAGAAGGAAACCGAGGAAACGCAATA
89	ATAACGGAATACCCAAAAGAACTGGCATGATTAAGACT
90	CCTTATTACGCAGTATGTTAGCAAACGTAGAAAATACA

91	TACATAAAGGTGGCAACATATAAAAGAAACGCAAAGAC
92	ACCACGGAATAAGTTTATTTTGTCACAATCAATAGAAA
93	ATTCATATGGTTTACCAGCGCCAAAGACAAAAGGGCGA
94	CATTCAACCGATTGAGGGAGGGAAGGTAAATATTGACG
95	GAAATTATTCATTAAAGGTGAATTATCACCGTCACCGA
96	CTTGAGCCATTTGGGAATTAGAGCCAGCAAAATCACCA
97	GTAGCACCATTACCATTAGCAAGGCCGGAAACGTCACC
98	AATGAAACCATCGATAGCAGCACCGTAATCAGTAGCGA
99	CAGAATCAAGTTTGCCTTTAGCGTCAGACTGTAGCGCG
100	TTTTCATCGGCATTTTCGGTCATAGCCCCCTTATTAGC
101	GTTTGCCATCTTTTCATAATCAAAATCACCGGAACCAG
102	AGCCACCACCGGAACCGCCTCCCTCAGAGCCGCCACCC
103	TCAGAACCGCCACCCTCAGAGCCACCACCCTCAGAGCC
104	GCCACCAGAACCACCACCAGAGCCGCCGCCAGCATTGA
105	CAGGAGGTTGAGGCAGGTCAGACGATTGGCCTTGATAT
106	TCACAAACAAATAAATCCTCATTAAAGCCAGAATGGAA
107	AGCGCAGTCTCTGAATTTACCGTTCCAGTAAGCGTCAT
108	ACATGGCTTTTGATGATACAGGAGTGTACTGGTAATAA
109	GTTTTAACGGGGTCAGTGCCTTGAGTAACAGTGCCCGT
110	ATAAACAGTTAATGCCCCCTGCCTATTTCGGAACCTAT
111	TATTCTGAAACATGAAAGTATTAAGAGGCTGAGACTCC
112	TCAAGAGAAGGATTAGGATTAGCGGGGTTTTGCTCAGT
113	ACCAGGCGGATAAGTGCCGTCGAGAGGGTTGATATAAG
114	TATAGCCCGGAATAGGTGTATCACCGTACTCAGGAGGT
115	TTAGTACCGCCACCCTCAGAACCGCCACCCTCAGAACC
116	GCCACCCTCAGAGCCACCACCCTCATTTTCAGGGATAG
117	CAAGCCCAATAGGAACCCATGTACCGTAACACTGAGTT
118	TCGTCACCAGTACAAACTACAACGCCTGTAGCATTCCA
119	CAGACAGCCCTCATAGTTAGCGTAACGATCTAAAGTTT
120	TGTCGTCTTTCCAGACGTTAGTAAATGAATTTTCTGTA
121	TGGGATTTTGCTAAACAACTTTCAACAGTTTCAGCGGA
122	GTGAGAATAGAAAGGAACAACTAAAGGAATTGCGAATA
123	ATAATTTTTTCACGTTGAAAATCTCCAAAAAAAAGGCT
124	CCAAAAGGAGCCTTTAATTGTATCGGTTTATCAGCTTG
125	CTTTCGAGGTGAATTTCTTAAACAGCTTGATACCGATA
126	GTTGCGCCGACAATGACAACAACCATCGCCCACGCATA
127	ACCGATATATTCGGTCGCTGAGGCTTGCAGGGAGTTAA
128	AGGCCGCTTTTGCGGGATCGTCACCCTCAGCAGCGAAA
129	GACAGCATCGGAACGAGGGTAGCAACGGCTACAGAGGC
130	TTTGAGGACTAAAGACTTTTTCATGAGGAAGTTTCCAT
131	TAAACGGGTAAAATACGTAATGCCACTACGAAGGCACC
132	AACCTAAAACGAAAGAGGCAAAAGAATACACTAAAACA
133	CTCATCTTTGACCCCCAGCGATTATACCAAGCGCGAAA
134	CAAAGTACAACGGAGATTTGTATCATCGCCTGATAAAT
135	TGTGTCGAAATCCGCGACCTGCTCCATGTTACTTAGCC
136	GGAACGAGGCGCAGACGGTCAATCATAAGGGAACCGAA
137	CTGACCAACTTTGAAAGAGGACAGATGAACGGTGTACA

138	GACCAGGCGCATAGGCTGGCTGACCTTCATCAAGAGTA
139	ATCTTGACAAGAACCGGATATTCATTACCCAAATCAAC
140	GTAACAAAGCTGCTCATTCAGTGAATAAGGCTTGCCCT
141	GACGAGAAACACCAGAACGAGTAGTAAATTGGGCTTGA
142	GATGGTTTAATTTCAACTTTAATCATTGTGAATTACCT
143	TATGCGATTTTAAGAACTGGCTCATTATACCAGTCAGG
144	ACGTTGGGAAGAAAAATCTACGTTAATAAAACGAACTA
145	ACGGAACAACATTATTACAGGTAGAAAGATTCATCAGT
146	TGAGATTTAGGAATACCACATTCAACTAATGCAGATAC
147	ATAACGCCAAAAGGAATTACGAGGCATAGTAAGAGCAA
148	CACTATCATAACCCTCGTTTACCAGACGACGATAAAAA
149	CCAAAATAGCGAGAGGCTTTTGCAAAAGAAGTTTTGCC
150	AGAGGGGGTAATAGTAAAATGTTTAGACTGGATAGCGT
151	CCAATACTGCGGAATCGTCATAAATATTCATTGAATCC
152	CCCTCAAATGCTTTAAACAGTTCAGAAAACGAGAATGA
153	CCATAAATCAAAAATCAGGTCTTTACCCTGACTATTAT
154	AGTCAGAAGCAAAGCGGATTGCATCAAAAAGATTAAGA
155	GGAAGCCCGAAAGACTTCAAATATCGCGTTTTAATTCG
156	AGCTTCAAAGCGAACCAGACCGGAAGCAAACTCCAACA
157	GGTCAGGATTAGAGAGTACCTTTAATTGCTCCTTTTGA
158	TAAGAGGTCATTTTTGCGGATGGCTTAGAGCTTAATTG
159	CTGAATATAATGCTGTAGCTCAACATGTTTTAAATATG
160	CAACTAAAGTACGGTGTCTGGAAGTTTCATTCCATATA
161	ACAGTTGATTCCCAATTCTGCGAACGAGTAGATTTAGT
162	TTGACCATTAGATACATTTCGCAAATGGTCAATAACCT
163	GTTTAGCTATATTTTCATTTGGGGCGCGAGCTGAAAAG
164	GTGGCATCAATTCTACTAATAGTAGTAGCATTAACATC
165	CAATAAATCATACAGGCAAGGCAAAGAATTAGCAAAAT
166	TAAGCAATAAAGCCTCAGAGCATAAAGCTAAATCGGTT
167	GTACCAAAAACATTATGACCCTGTAATACTTTTGCGGG
168	AGAAGCCTTTATTTCAACGCAAGGATAAAAATTTTTAG
169	AACCCTCATATATTTTAAATGCAATGCCTGAGTAATGT
170	GTAGGTAAAGATTCAAAAGGGTGAGAAAGGCCGGAGAC
171	AGTCAAATCACCATCAATATGATATTCAACCGTTCTAG
172	CTGATAAATTAATGCCGGAGAGGGTAGCTATTTTTGAG
173	AGATCTACAAAGGCTATCAGGTCATTGCCTGAGAGTCT
174	GGAGCAAACAAGAGAATCGATGAACGGTAATCGTAAAA
175	CTAGCATGTCAATCATATGTACCCCGGTTGATAATCAG
176	AAAAGCCCCAAAAACAGGAAGATTGTATAAGCAAATAT
177	TTAAATTGTAAACGTTAATATTTTGTTAAAATTCGCAT
178	TAAATTTTTGTTAAATCAGCTCATTTTTTAACCAATAG
179	GAACGCCATCAAAAATAATTCGCGTCTGGCCTTCCTGT
180	AGCCAGCTTTCATCAACATTAAATGTGAGCGAGTAACA
181	ACCCGTCGGATTCTCCGTGGGAACAAACGGCGGATTGA
182	CCGTAATGGGATAGGTCACGTTGGTGTAGATGGGCGCA
183	TCGTAACCGTGCATCTGCCAGTTTGAGGGGACGACGAC
184	AGTATCGGCCTCAGGAAGATCGCACTCCAGCCAGCTTT

185	CCGGCACCGCTTCTGGTGCCGGAAACCAGGCAAAGCGC
186	CATTCGCCATTCAGGCTGCGCAACTGTTGGGAAGGGCG
187	ATCGGTGCGGGCCTCTTCGCTATTACGCCAGCTGGCGA
188	AAGGGGGATGTGCTGCAAGGCGATTAAGTTGGGTAACG
189	CCAGGGTTTTCCCAGTCACGACGTTGTAAAACGACGGC
190	CAGTGCCAAGCTTGCATGCCTGCAGGTCGACTCTAGAGGATCTTTT

Supplementary Table S3. Oligonucleotides were replaced from Table S2 to assemble reference structures. The DNA dumbbell forming sequence is indicated in red.

Name	Sequence (5' → 3')	Length (nt)	# of oligos replaced
REF 1.1	ACATCACTTGCCTGAGTAGA	20	26-30

REF 1.2	AGAACTCAAATCCTCTTTTGAGGAACAAGTTTTCTTGTCTATCGGCCT	48	
REF 1.3	TGCTGGTAATTCCTCTTTTGAGGAACAAGTTTTCTTGTATCCAGAACA	48	
REF 1.4	ATATTACCGCTCCTCTTTTGAGGAACAAGTTTTCTTGTCAGCCATTGC	48	
REF 1.5	AACAGGAAAATCCTCTTTTGAGGAACAAGTTTTCTTGTACGCTCATGG	48	
REF 1.6	AAATACCTACTCCTCTTTTGAGGAACAAGTTTTCTTGTATTTTGACGC	48	
REF 1.7	TCAATCGTCTTCCTCTTTTGAGGAACAAGTTTTCTTGTGAAATGGATT	48	
REF 1.8	ATTTACATTGGCAGATTCAC	20	
REF 1.9	CAGTCACACGACCAGTAATAAAAGGGACAT	30	
REF 2.1	TCACAAACAAATAAATCCTCATTAAAGCCAGAATGGAAAGCGCAGTCTCTGAATTT	56	106-112
REF 2.2	ACCGTTCCAGTAAGCGTCAT	20	
REF 2.3	ACATGGCTTTTCCTCTTTTGAGGAACAAGTTTTCTTGTTGATGATACA	48	
REF 2.4	GGAGTGTACTTCCTCTTTTGAGGAACAAGTTTTCTTGTGGTAATAAGT	48	
REF 2.5	TTTAACGGGGTCCTCTTTTGAGGAACAAGTTTTCTTGTTCAGTGCCTT	48	
REF 2.6	GAGTAACAGTTCCTCTTTTGAGGAACAAGTTTTCTTGTGCCCGTATAA	48	
REF 2.7	ACAGTTAATGTCCTCTTTTGAGGAACAAGTTTTCTTGTCCCCCTGCCT	48	
REF 2.8	ATTTCGGAACTCCTCTTTTGAGGAACAAGTTTTCTTGTCTATTATTCT	48	
REF 2.9	GAAACATGAAAGTATTAAGA	20	
REF 2.10	GGCTGAGACTCCTCAAGAGAAGGATTAGGATTAGCGGGGTTTTGCTCAGT	50	

Section S4. AFM imaging

Section 4.1 Sample preparation and imaging with AFM

Atomic Force Microscopy (Nanosurf Mobile S) imaging of nanobaits was performed in the air in a non-contact mode. All scans were performed on a bare mica surface following the adsorption of nanobaits as follows. We placed a 10 μL drop of a DNA solution (diluted to 1 ng/μL in filtered 10 mM $MgCl_2$ and 10 mM Tris-HCl, pH 8.0) onto a freshly cleaved mica surface for 1 minute, rinsed the mica plate three times with 100 μL of Mili-Q water and then blow-dried it with Nitrogen. Before the scan, the mica plate was affixed to the AFM sample stage using double-sided adhesive tape. Image visualization and analysis were done using Gwyddion.

Section 4.2 AFM images of nanobait

AFM images of nanobait are shown in Figures S3 and S4. Figure S3a presents AFM images of the nanobait structure without any label added. In some cases, two references are visible (circled in dark grey, Figure S3a, right). However, it is known that DNA dumbbell structures are hardly distinguishable with AFM imaging in comparison to nanopores [1].

Nanobait events with monovalent streptavidin (Figure S3b) indicate five structures that correspond to capture sites with labels, as expected from the nanobait design. The same design but with the DNA flower label is presented in Figure S4. The DNA flower is larger than streptavidin and hence easier to be detected using AFM imaging (Figure S2).

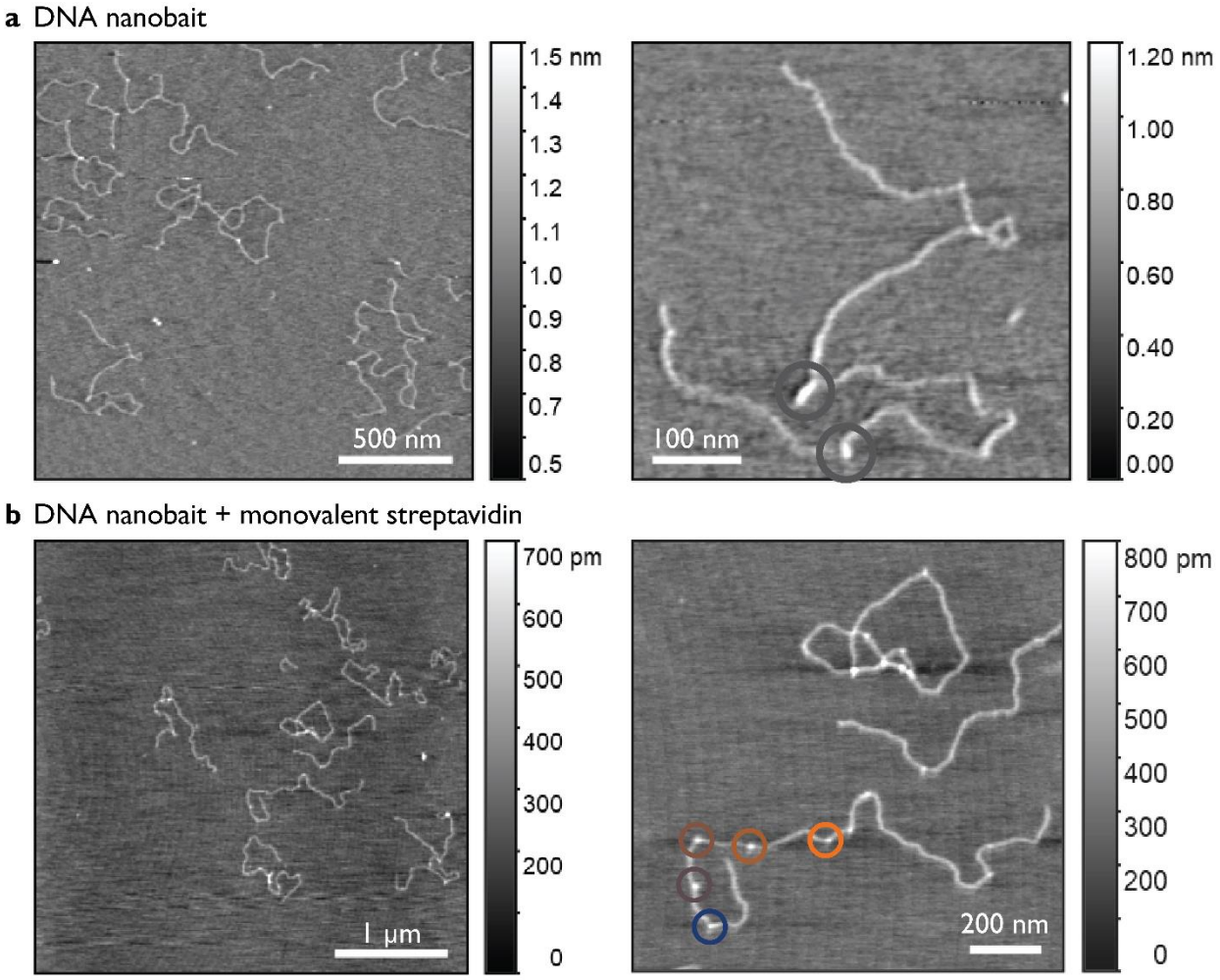

Figure S3. AFM images of DNA nanobait (as in Figure 3) with monovalent streptavidin. a) Nanobait without monovalent streptavidin has two reference structures (circled in dark gray). b) AFM images of nanobait with monovalent streptavidin used as a label. Five capture sites are circled in corresponding colors. Five non-overlapping areas are imaged for each sample.

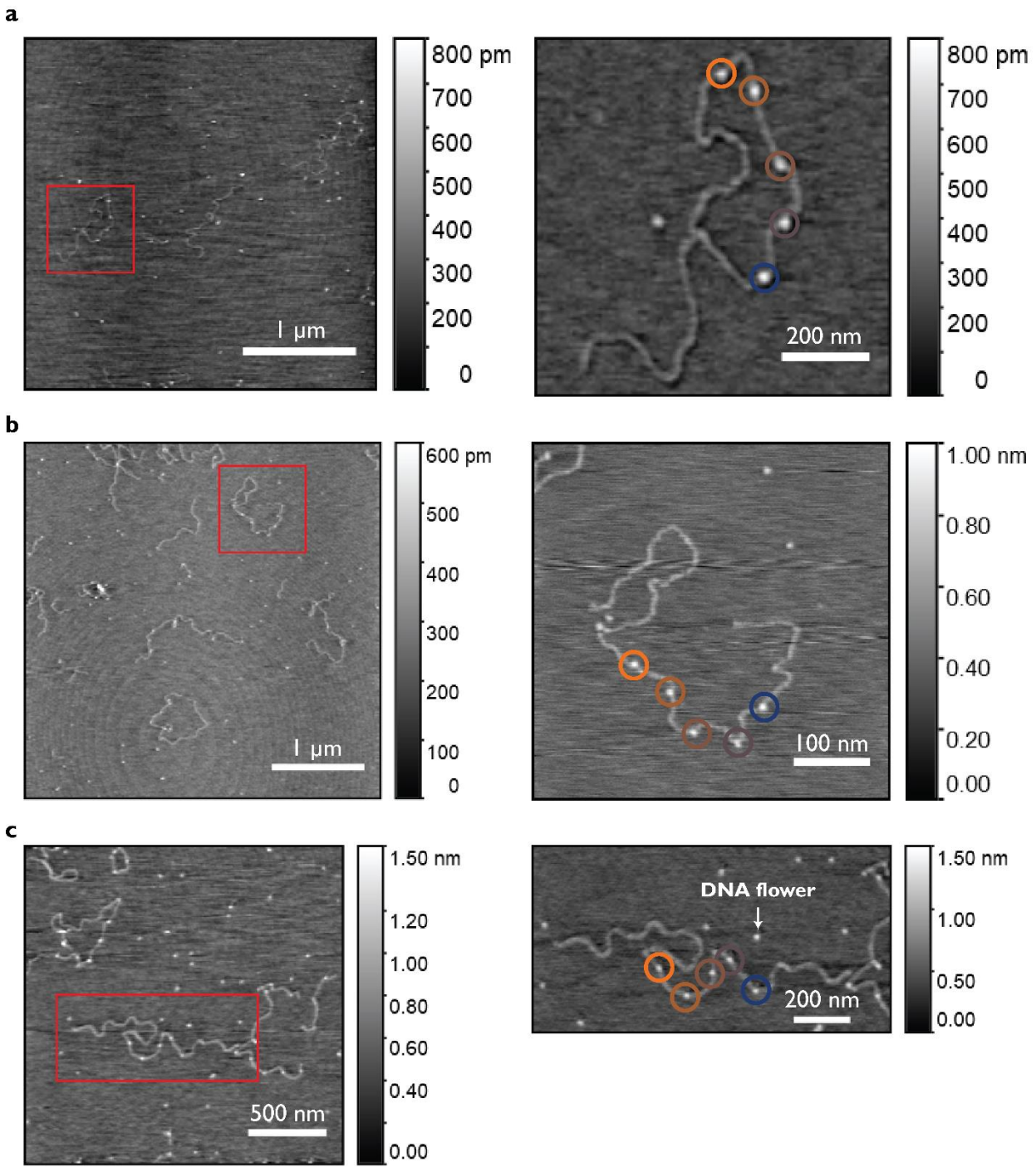

Figure S4. AFM images of nanobait (as in Figure 3) with DNA flower as a label. Three different nanobait example images are shown in a), b), and c). Five non-overlapping areas are imaged for each sample.

Section S5. EMSA analysis

We performed the electrophoretic mobility shift assay (EMSA) to see a mobility shift caused by streptavidin binding to all five sites on nanobait (Figure S5). 2 % (w/v) agarose (BioReagent, low electroendosmosis, Merck SigmaAldrich; catalog number A9539) gel was prepared by adding 2 g of agarose, 10 mL of 10 × Tris-Borate-EDTA buffer (TBE buffer), and Milli-Q water was added to 100 mL. The gel was heated in the microwave at the maximum power (800 W) for 2-3 min. It was cooled down and poured into a gel tray to set for 45 min.

Samples were mixed with purple gel loading dye (New England Biolabs; catalog number B7025S) and TBE buffer to 1 × with ~150 ng of a DNA sample. We used a 1 kb DNA ladder as a reference (New England Biolabs; catalog number N3232) with a size range from 500 bp to 10 kb (Figure S5a). Nanobait in lane 2 (Figure S5a) was mixed with 10 × excess of wild-type tetravalent streptavidin (ThermoFisher Scientific; catalog number 21125).

It can be observed from the agarose gel in Figure S5a that there is a slight shift from nanobait (lane 1) to nanobait + streptavidin (lane 2). We used gel intensity analysis using an open-source software Fiji[8] to plot this shift, indicating that streptavidin(s) is bound to nanobait (Figure S5b).

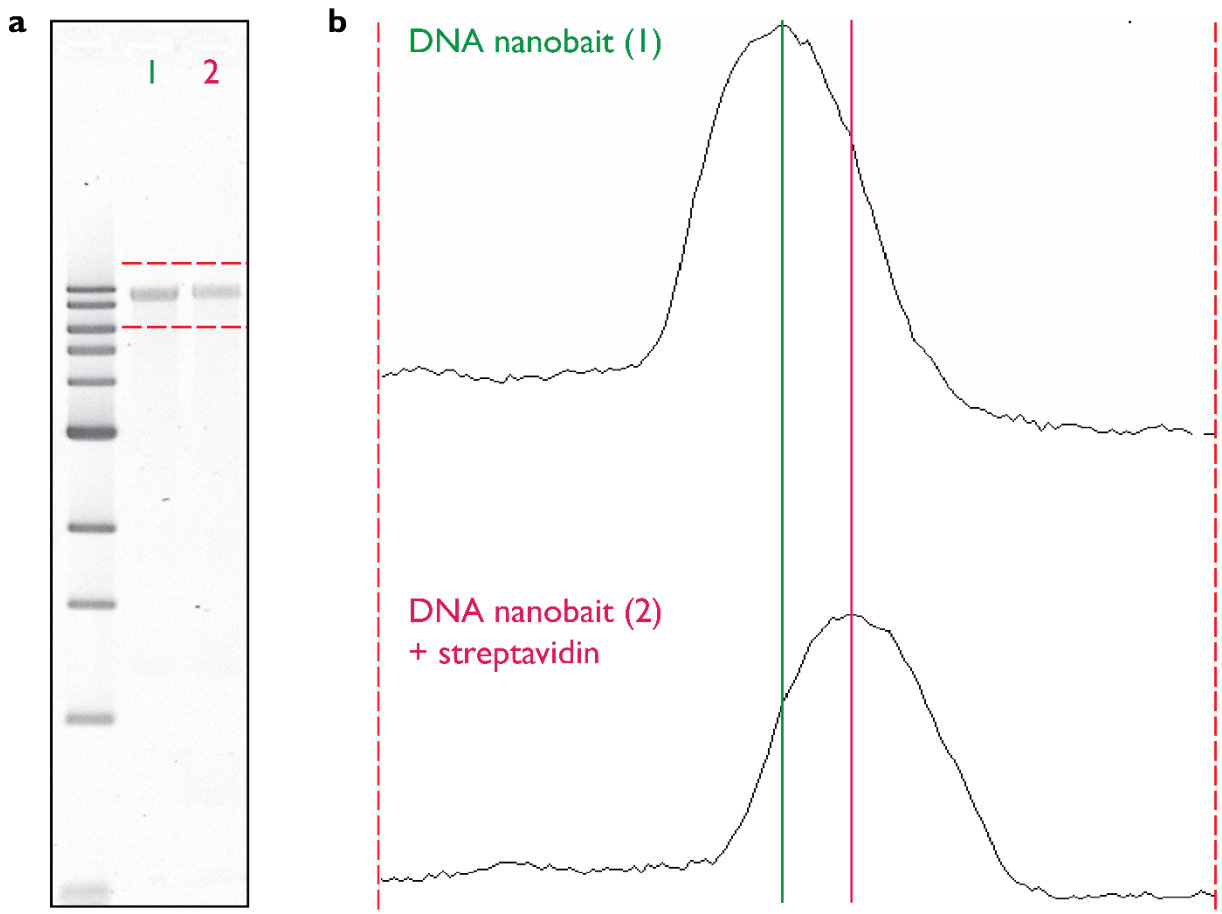

Figure S5. Electrophoretic mobility shift assay (EMSA) of nanobait without and with streptavidin. a) 2% (w/v) agarose gel od nanobait without (lane 1) and with (lane 2) streptavidin added. We used a 1 kb DNA ladder (New England Biolabs; product number N3232). The two top lines of the ladder are 10 and 8 kb. b) The intensity traces of corresponding lanes from a). The green line indicates the intensity maximum of nanobait (lane 1) and the purple line indicates the intensity maximum of nanobait + streptavidin (lane 2). The shift between the green and purple lines corresponds to streptavidin(s) bound to capture sites on nanobait. Samples were run once.

Section S6. Multiple respiratory viruses DNA nanobait sequences and example events

Nanobait for multiple respiratory viruses is prepared as previously described in Section S2. Below, are listed sequences of capture sites (Table S7), biotin strand (Table S6), and target sequence (Table S5) for each virus.

We also show here additional nanopore events of nanobait without target added (Figure S6a), with SARS-CoV-2 target (Figure S6b), Influenza A (Figure S6c), RSV (Figure S6d), Parainfluenza (Figure S6e), and Rhinoviruses (Figure S6f). Targets for Influenza A, Parainfluenza A, and Rhinoviruses target cohort rather than a single variant [9,10]. The nanobait and peaks resemble those presented in Figure 2a of the manuscript. These single-molecule events are obtained from three separate nanopore measurements.

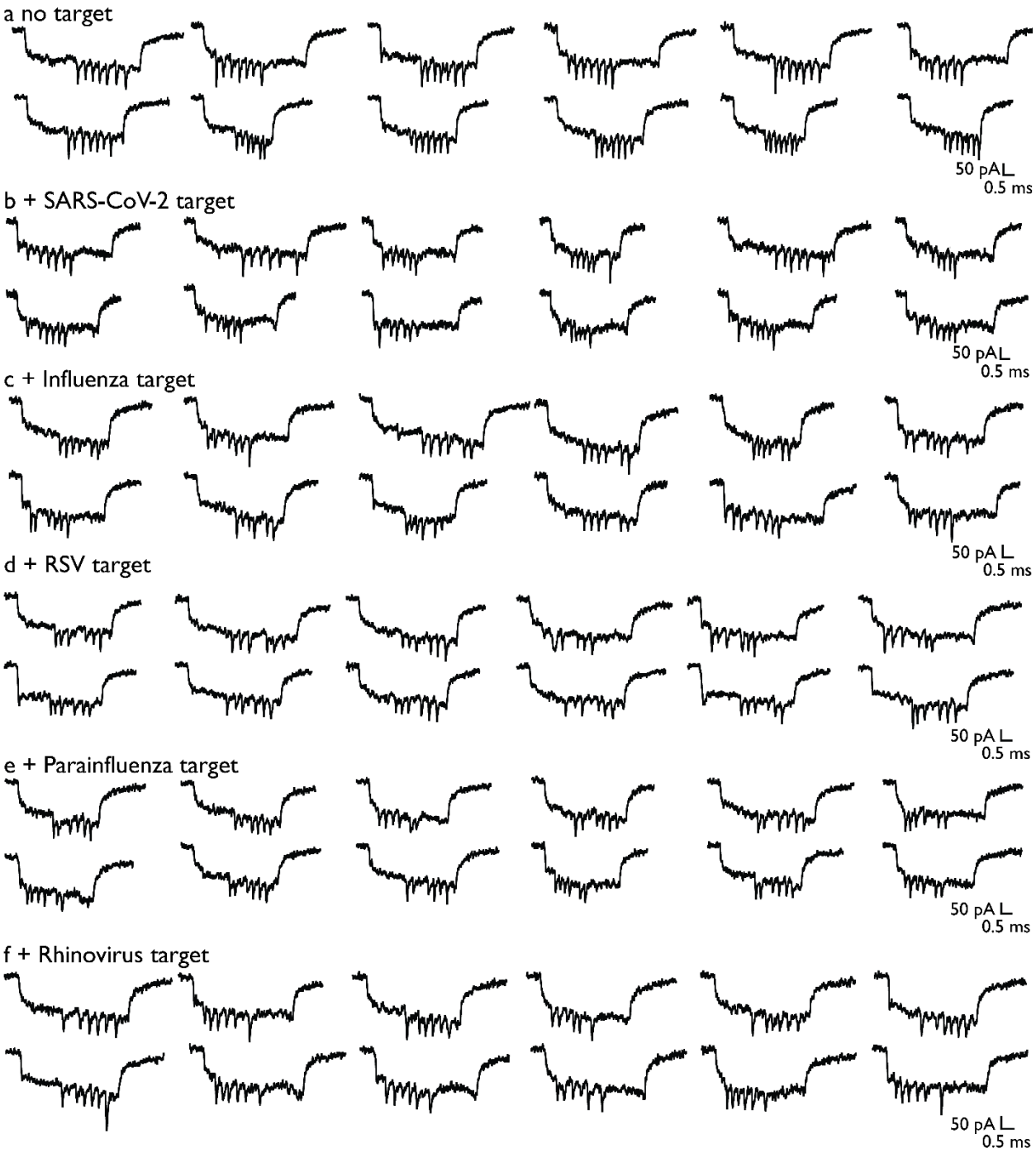

Figure S6. Additional example events for nanobait used for identification of various respiratory viruses with a) no target added, b) SARS-CoV-2 target, c) Influenza target, d) RSV, e) Parainfluenza target, and f) Rhinovirus target.

Supplementary Table S4. Presence of peaks at their respective sites for multiple virus identification.

Target/Case	Control (no targets)	Standard error	Target present	Standard error
SARS-CoV-2	0.17	0.04	0.75	0.10
RSV	0.09	0.01	0.96	0.06
Rhinovirus	0.08	0.03	0.89	0.13
Influenza	0.11	0.04	0.49	0.17
Parainfluenza	0.03	0.01	0.73	0.04

Supplementary Table S5. Target sequences for multiple virus identification.

Strand name	Virus / group of viruses	Sequence reference	Sequence (5' → 3')
SW	SARS-CoV-2_Reference	NCBI Reference Sequence: NC_045512.2[11]	GTATGAAAATGCCTTTTTAC
Infl	Influenza A viruses universal	Sequence adapted from[12]	TGACAGGATTGGTCTTGTCT
RSV	Respiratory syncytial virus universal A	Sequence adapted from[13]	ACACAGCAGCTGTTCAGTAC
PI	Parainfluenza 1	Sequence adapted from[10]	CTTCCTGCTGGTGTGTTAAT
RV	Rhinoviruses universal	Sequence adapted from[9]	TCCTCCGGCCCCTGAATGTG

Supplementary Table S6. 3' biotinylated strand sequences for multiple virus identification.

Strand name	Virus / group of viruses	Sequence (5' → 3')
bSW	SARS-CoV-2_Reference	AAATGCCTTTTTAC/3-biotin/
bInfl	Influenza A viruses universal	GATTGGTCTTGTCT/3-biotin/
bRSV	Respiratory syncytial virus universal A	CAGCTGTTCAGTAC/3-biotin/
bPI	Parainfluenza 1	GCTGGTGTGTTAAT/3-biotin/

bRV	Rhinoviruses universal	GGCCCCTGAATGTG /3-biotin/

Supplementary Table S7. Capture strand sequences for multiple virus identification.

Strand name	Virus / group of viruses	Sequence (5' → 3')
cSW_42	SARS-CoV-2_Reference	TTCGACAACTCGTATTAAATCCTTTGCCCGAACGTTAT TTTTT GTAAAAAGGCATTTTCATAC
cRSV_55	Respiratory syncytial virus universal A	GTGAGTGAATAACCTTGCTTCTGTAAATCGTCGCTATT TTTTT GTACTGAACAGCTGCTGTGT
cRV_68	Rhinoviruses universal	AGAATATAAAGTACCGACAAAAGGTAAAGTAATTCTGT TTTTT CACATTCAGGGGCCGGAGGA
cI_81	Influenza A viruses universal	TCCCAATCCAAATAAGAAACGATTTTTTGTTTAACGTC TTTTT AGACAAGACCAATCCTGTCA
cPI_94	Parainfluenza 1	CATTCAACCGATTGAGGGAGGGAAGGTAAATATTGACG TTTTT ATTAACACACCAGCAGGAAG

Section S7. Multiple SARS-Co-V-2 virus variants DNA nanobait sequences and example events

Nanobait for multiple SARS-CoV-2 variants was prepared as previously described in Section S2. Below are listed sequences of capture sites (Table S12), biotin strand (Table S10), and target sequence of the wildtype (Table S11) and variant (Table S9).

We also showed here additional nanopore events of nanobait without target added (Figure S7a), with B reference target (Figure S7b), B.1.617 variant target (Figure S7c), B.1 variant target (Figure S7d), B.1.1.7 variant target (Figure S7e), and B.1.351 variant target (Figure S7f). The nanobait and peaks resembled those presented in Figure 2b of the manuscript. These single-molecule events were obtained from three separate nanopore measurements.

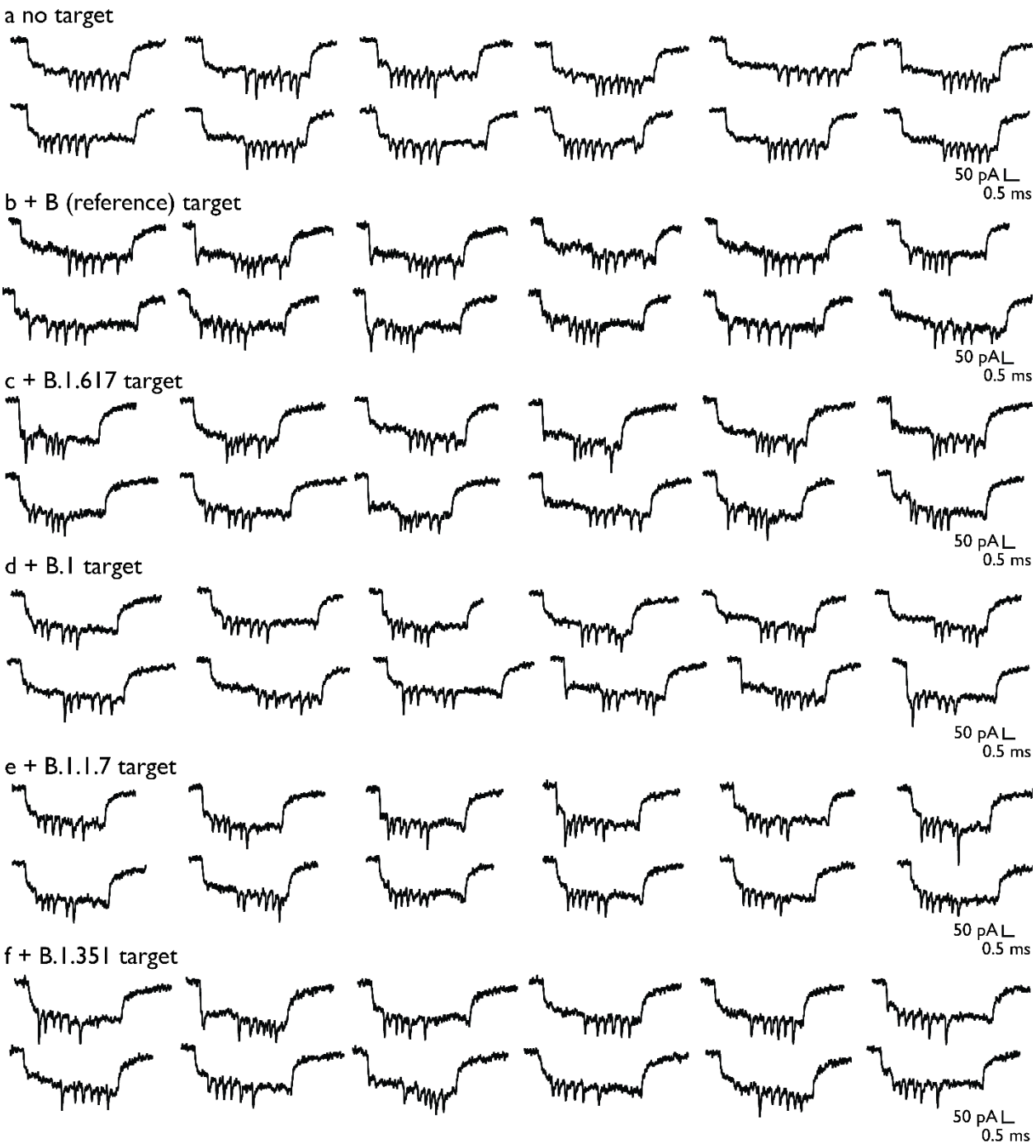

Figure S7. Additional example events for nanobait used for identification of various SARS-CoV-2 variants with a) no target added, b) B target, c) B.1.617 variant target, d) B.1 variant target, e) B.1.1.7 variant target, and f) B.1.351 variant target.

Supplementary Table S8. Presence of peaks at their respective sites for multiple variant identification.

Target/Case	Control (no targets)	Standard error	WT target present	Standard error	Variant target present	Standard error
B (reference)	0.08	0.00	0.93	0.04	0.92	0.06
B.1.617 (Delta)	0.23	0.01	0.39	0.02	0.77	0.01
B.1	0.02	0.00	0.29	0.05	0.98	0.06
B.1.1.7 (Alpha)	0.04	0.00	0.06	0.02	0.96	0.12
B.1.351 (Beta)	0.10	0.00	0.49	0.11	0.90	0.03

Supplementary Table S9. Target sequences for multiple SARS-CoV-2 variant identification. In red, single nucleotide variant positions are highlighted, while yellow highlights the toehold region used for the SDR.

Strand name	WHO nomenclature[14]	Pangolin nomenclature[15]	Single nucleotide variation	Sequence (5' → 3')
SW	Reference	B (reference)	/	GTATGAAAATGCCTTTTTAC
SIm	Delta	B.1.617	T-G L452R	CCGGTATAGATTGTTTAGGA
SEm	NA	B.1	A-G D614G	GGTGTTAACTGCACAGAAGT
SUKm	Alpha	B.1.1.7	A-T N501Y	CTTATGGTGTTGGTTACCAA
SSAm	Beta	B.1.351	G-A E484K	TAAAGGTTTTAATTGTTACT

Supplementary Table S10. 3' biotinylated strand sequences for multiple SARS-CoV-2 variant identification.

Strand name	Variant name	Sequence (5’ → 3’)
bSW	B (reference)	AAATGCCTTTTTAC/3-BIOTIN/
bSIm	B.1.617 (Delta)	TAGATTGTTTAGGA/3-BIOTIN/
bSEm	B.1	AACTGCACAGAAGT/3-BIOTIN/
bSUKm	B.1.1.7 (Alpha)	GTGTTGGTTACCAA/3-BIOTIN/
bSSAm	B.1.351 (Beta)	TTTTAATTGTTACT/3-BIOTIN/

Supplementary Table S11. Wild-type (WT) target sequences for multiple SARS-CoV-2 variant identification. In green, wild-type nucleotide positions are highlighted, while yellow highlights the toehold region used for the SDR.

Strand name	Sequence (5’ → 3’)	Length (nt)
SI	CCTGTATAGATTGTTTAGGA	20
SE	GATGTTAACTGCACAGAAGT	20
SUK	CTAATGGTGTTGGTTACCAA	20
SSA	TGAAGGTTTTAATTGTTACT	20

Supplementary Table S12. Capture strand sequences for multiple SARS-CoV-2 variant identification.

Strand name	Variant name	Sequence (5’ → 3’)
cSW_42	B (reference)	TTCGACAACTCGTATTAAATCCTTTGCCCGAACGTTAT TTTTT GTAAAAAGGCATTTTCATAC
cSI_68	B.1.617 (Delta)	AGAATATAAAGTACCGACAAAAGGTAAAGTAATTCTGT TTTTT TCCTAAACAATCTATACCGG
cSE_94	B.1	CATTCAACCGATTGAGGGAGGGAAGGTAAATATTGACG TTTTT ACTTCTGTGCAGTTAACACC
cSUK_81	B.1.1.7 (Alpha)	TCCCAATCCAAATAAGAAACGATTTTTTGTTTAACGTC TTTTT TTGGTAACCAACACCATAAG

cSSA_55	B.1.351 (Beta)	GTGAGTGAATAACCTTGCTTCTGTAAATCGTCGCTATT TTTTT AGTAACAATTAAAACCTTTA

Section S8. Discrimination of control SARS-Co-V-2 RNA virus variants

Nanobait for SARS-CoV-2 N501 RNA virus variants was prepared as previously described in Section S2 (Figure S8). Below, are listed sequences of SARS-CoV-2 N501 RNA, capture sites, biotinylated strand, and guide oligos used for RNase H cutting (Table S13).

Programmable RNase H cutting of SARS-CoV-2 RNA controls for nanobait

For nanopore sensing, SARS-CoV-2 RNA (S:N501 in Table S13) controls were used for the detection with nanobait. Firstly, we mixed guide oligos with a SARS-CoV-2 N501 RNA in the ratio 1:1:1 and heated the mixture to 70 °C for 5 minutes. RNase H (5,000 units/ml, NEB) was added, mixed, and heated for 20 minutes at 37 °C to allow the enzyme to cut RNA in the DNA : RNA hybrid that effectively leads to the release of target RNA. RNase H is thermally inactivated by incubation at 65 °C for 10 min.

Nanopore readout of DNA nanobait

Nanobait was mixed with a cut long RNA control at ten times excess in 10 mM $MgCl_2$ and 100 mM NaCl. The mixture (5 µL) was incubated at room temperature (~10 min) until prepared for nanopore measurement.

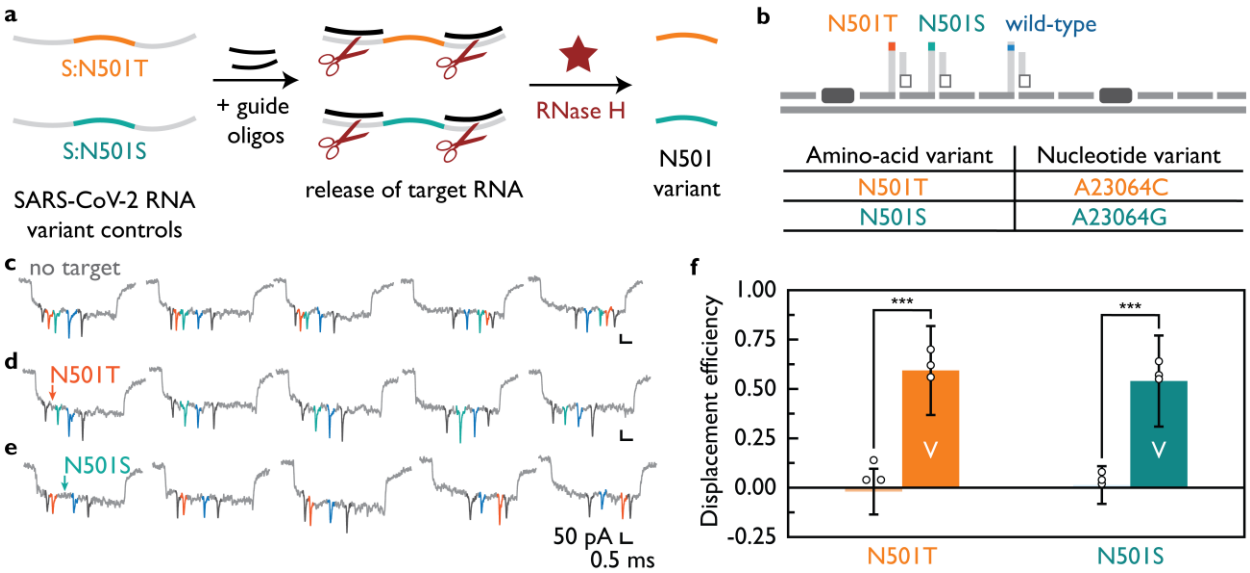

Figure S8. Nanobait discriminates single-nucleotide SARS-CoV-2 RNA variants. a) SARS-CoV-2 RNA variant controls that have one amino-acid substitutions. Guide oligos are added next to the target RNA sequence hence enabling RNase H cutting and releasing of target RNAs in solution. b) Nanobait design has two references, two sites for each of variant (N501T, N501S) and a wild-type site. In the table each of these amino-acid variants are shown with position and substitution of nucleotide counterpart indicated. c)

Example events for no target control indicate the correct number of downward spikes each corresponding to a structure depicted in b). In d) and e) are shown example events for each of the N501 variants. The absence of the colored spike indicates the presence of each respective target. f) Displacement efficiencies for single-nucleotide SARS-CoV-2 variants (labelled as 'V') are compared with the displacement efficiency for the wild-type SARS-CoV-2 (B.1.1.7). Error bars represent standard error and the center as the mean for three nanopore measurements and fifty nanopore events per measurement. The difference between conditions without and with variant targets is statistically significant (***p < 0.001; two-sided Student's T test; N=150).

Supplementary Table S13. SARS-CoV-2 RNA sequences and guide oligos, capture sites and biotinylated strands.

Strand name	Description	Sequence (5' → 3')
S:N501_RNA	Wild-type oligo	ATCATATGGTTTCCAACCCA CTTATGGTGTTGGTTACCAA CCATACAGAGTAGTAGTACT
S:N501T_RNA	A23064C	ATCATATGGTTTCCAACCCA CTTCTGGTGTTGGTTACCAA CCATACAGAGTAGTAGTACT
S:N501S_RNA	A23064G	ATCATATGGTTTCCAACCCA CTTGTGGTGTTGGTTACCAA CCATACAGAGTAGTAGTACT
Guide oligo S:N501_a	Downstream cutting oligo	TGGGTTGGAAACCATATGAT
Guide oligo S:N501_b	Upstream cutting oligo	AGTACTACTACTCTGTATGG
cS42:N501T	Carrier overhang	TTCGACAACTCGTATTAAATCCTTTGCCCGAACGTTAT TTTTT
cS55:N501S	Carrier overhang	GTGAGTGAATAACCTTGCTTCTGTAAATCGTCGCTATT TTTTT
cSUK_81	Carrier overhang	TCCCAATCCAAATAAGAAACGATTTTTTGTTTAACGTC TTTTT TTGGTAACCAACACCAAAAG
bS:N501	Biotin	GTGTTGGTTACCAA/3-BIOTIN/

Section S9. Kinetics of SDR with DNA and RNA targets

Nanobait for multiple SARS-CoV-2 targets is prepared as previously described in Section S2. Below, are listed sequences of capture sites (Table S17), biotin strands (Table S16), and target strands (Table S15).

Kinetics measurements for all five targets SDR are shown in Figure S9 and fifty nanobait events are analyzed per each data point. We tested targets of the same sequence but with different backbones as RNAs or DNAs (Figure S9a and S9b, respectively). Here, we show that target chemistry might have an effect on the kinetics of the SDR since some of the targets (e.g. target 3) have slower SDR for the RNA sequence than compared to the DNA sequence.

Additional nanopore events of nanobait without any target added (Figure S9c) and all five targets present (Figure S9d).

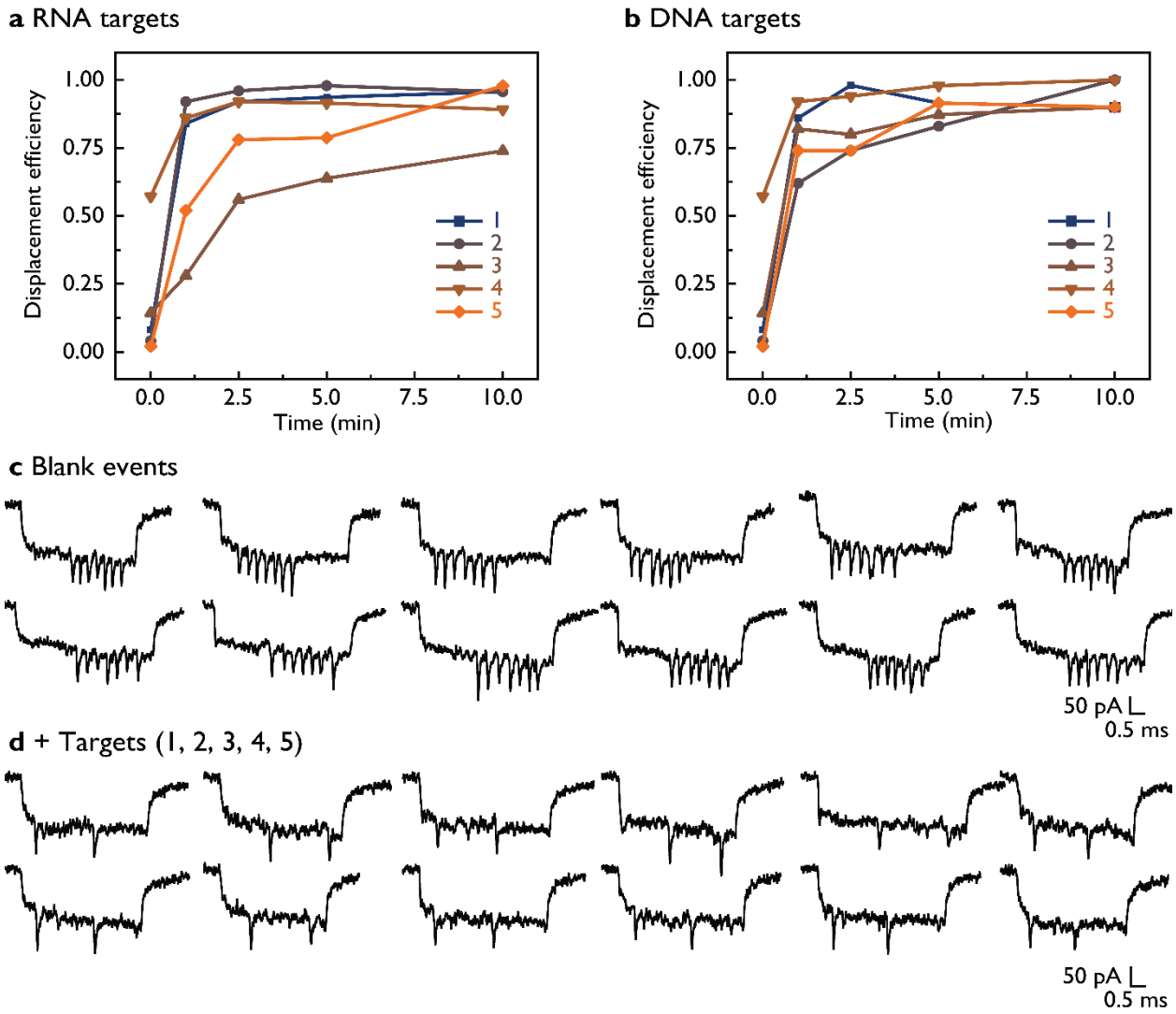

Figure S9. Kinetics of the toehold strand-displacement reaction (SDR) using RNA and DNA targets. Displacement efficiency for five different RNA or DNA targets is plotted in a) and b), respectively. c) Blank (no targets added) nanopore events indicate correct nanobait assembly. d) After the SDR with five targets added all five target-specific downward signals diminish.

We have measured single-molecule kinetics of SDR over 9 h for RNA targets (Figure S10). This experiment is performed with the diluted nanobait sample and in 1:1 ratio nanobait to target and allowed the typical 10 min incubation for the SDR. We have obtained from 1150 to 2860 events per hour slot (~18000 events) and the first fifty events were analyzed after each hour and the average value is plotted in Figure S10.

We can observe a general trend of increasing displacement efficiency for all five targets (Figure S10).

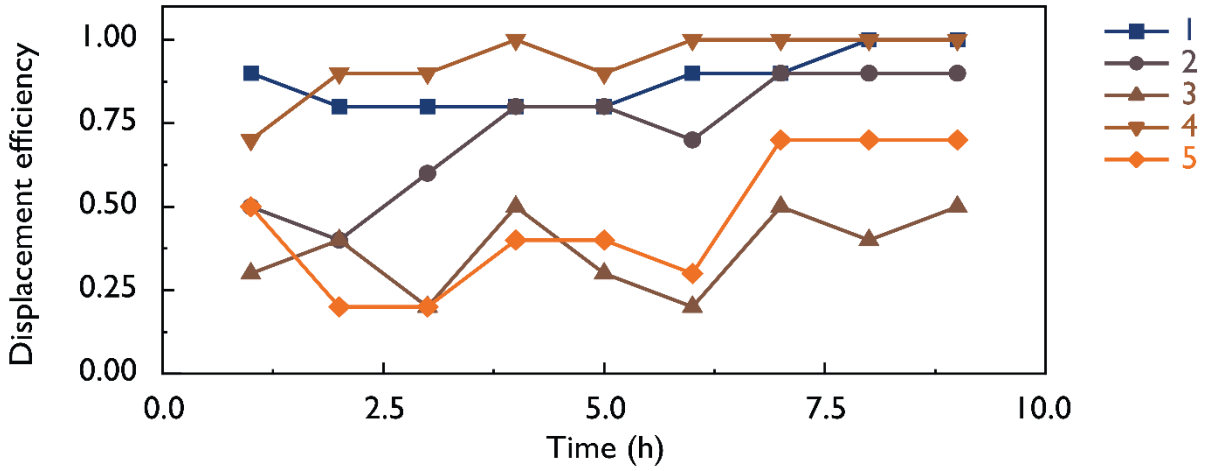

Figure S10. Single-molecule kinetics of the toehold strand-displacement reaction (SDR) using RNA targets.

Supplementary Table S14. Presence of peaks at their respective sites for multiple SARS-CoV-2 target identification.

Target/Case	Control (no targets)	Standard error	Target present	Standard error
H1	0.08	0.14	0.92	0.08
H2	0.10	0.16	0.90	0.22
H3	0.13	0.18	0.87	0.14
H4	0.38	0.11	0.62	0.08
H5	0.08	0.14	0.92	0.12

Supplementary Table S15. Target sequences for multiple SARS-CoV-2 target identification.

Strand name	Sequence (5' → 3')	Length (nt)

H1	TGATTGTGAAGAAGAAGAGT	20
H2	AAGAAAGGAGCTAAATTGTT	20
H3	AGAGTTGATTTTTGTGGAAA	20
H4	TGGTGTTTATTCTGTTATTT	20
H5	GGTAAAGTTGAGGGTTGTAT	20

Supplementary Table S16. 3’ Biotinylated strand sequences for SARS-CoV-2 target identification in a patient sample.

Strand name	Sequence (5’ → 3’)	Length (nt)
bH1	TGAAGAAGAAGAGT /3’-biotin/	14
bH2	GGAGCTAAATTGTT /3’-biotin/	14
bH3	GATTTTTGTGGAAA /3’-biotin/	14
bH4	TTATTCTGTTATTT /3’-biotin/	14
bH5	GTTGAGGGTTGTAT /3’-biotin/	14

Supplementary Table S17. Capture strand sequences for the multiple SARS-CoV-2 target identification.

Strand name	Sequence (5’ → 3’)	Length (nt)
cH1_42	TTCGACAACTCGTATTAAATCCTTTGCCCGAACGTTAT TTTTT ACTCTTCTTCTTCACAATCA	63
cH2_55	GTGAGTGAATAACCTTGCTTCTGTAAATCGTCGCTATT TTTTT AACAATTTAGCTCCTTTCTT	63
cH3_68	AGAATATAAAGTACCGACAAAAGGTAAAGTAATTCTGT TTTTT TTTCCACAAAAATCAACTCT	63

cH4_81	TCCCAATCCAAATAAGAAACGATTTTTTGTTTAACGTC TTTTT AAATAACAGAATAAACACCA	63
cH5_94	CATTCAACCGATTGAGGGAGGGAAGGTAAATATTGACG TTTTT ATACAACCCTCAACTTTACC	63

Section S10. Gel analysis of MS2 RNA cutting

Oligonucleotides A and B (Figure 4c) correspond to guide oligos TXA and TXB (X being the target name). Oligo C corresponds to cTX (X being the target name).

We treated MS2 RNA with a single target or with all three targets together to visualize site-specific cutting of RNA. We analyzed these samples using agarose gel electrophoresis (Figure S11). After MS2 RNA cutting for all three sites, we can observe expected lane mobility.

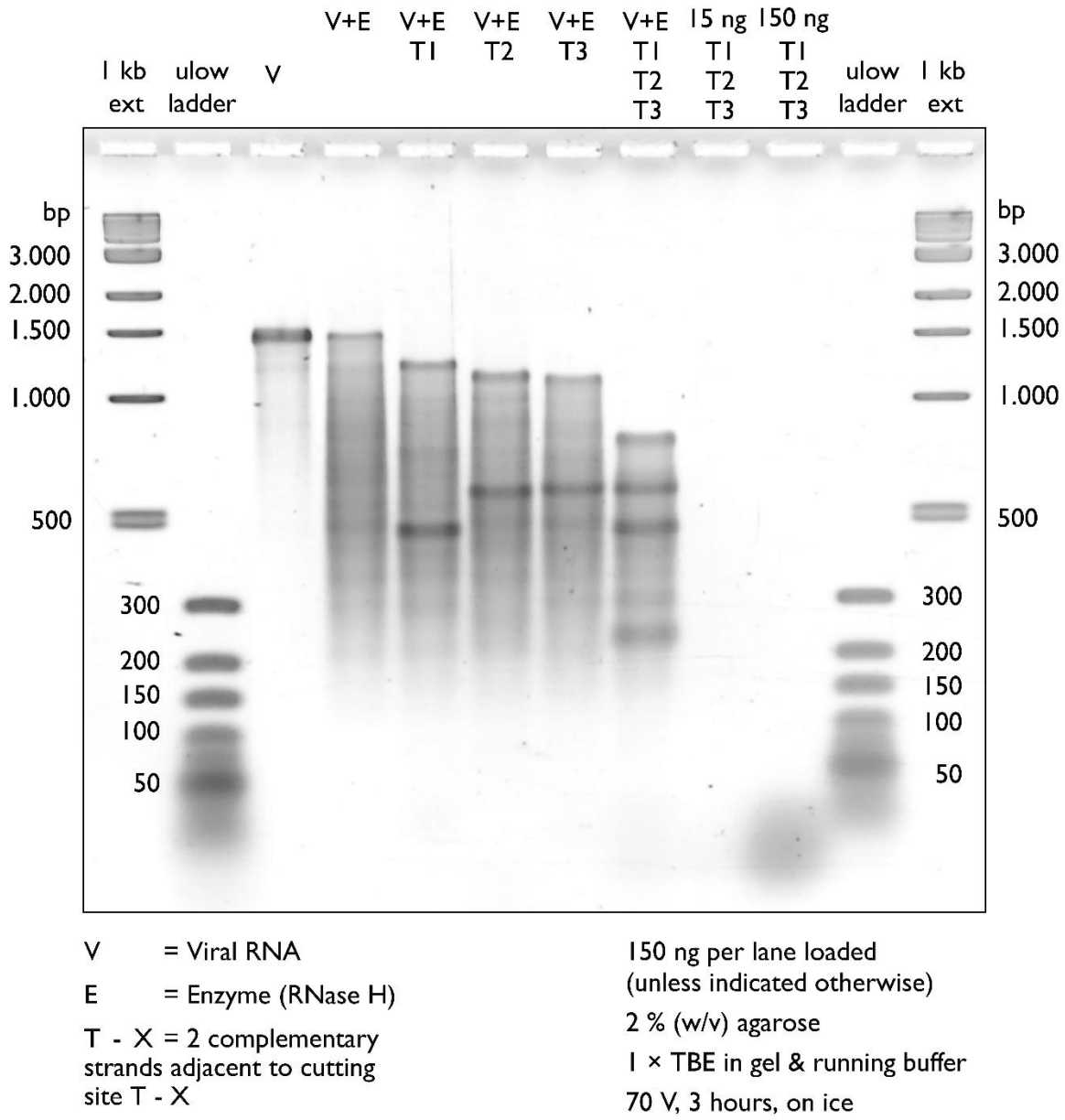

Figure S11. Agarose gel analysis of RNase H cutting of MS2 viral RNA.

We tested the mobility of targets, guide oligos, and capture oligos with non-denaturing polyacrylamide gel electrophoresis (PAGE) analysis (Figure S12). Despite targets and guide oligos having the same length they have different band mobility. This result indicates that mobility can be related to the sequence, given that this is the sole differentiating factor. We employed this advantage to detect each target in the background of guide oligos. Samples were run once.

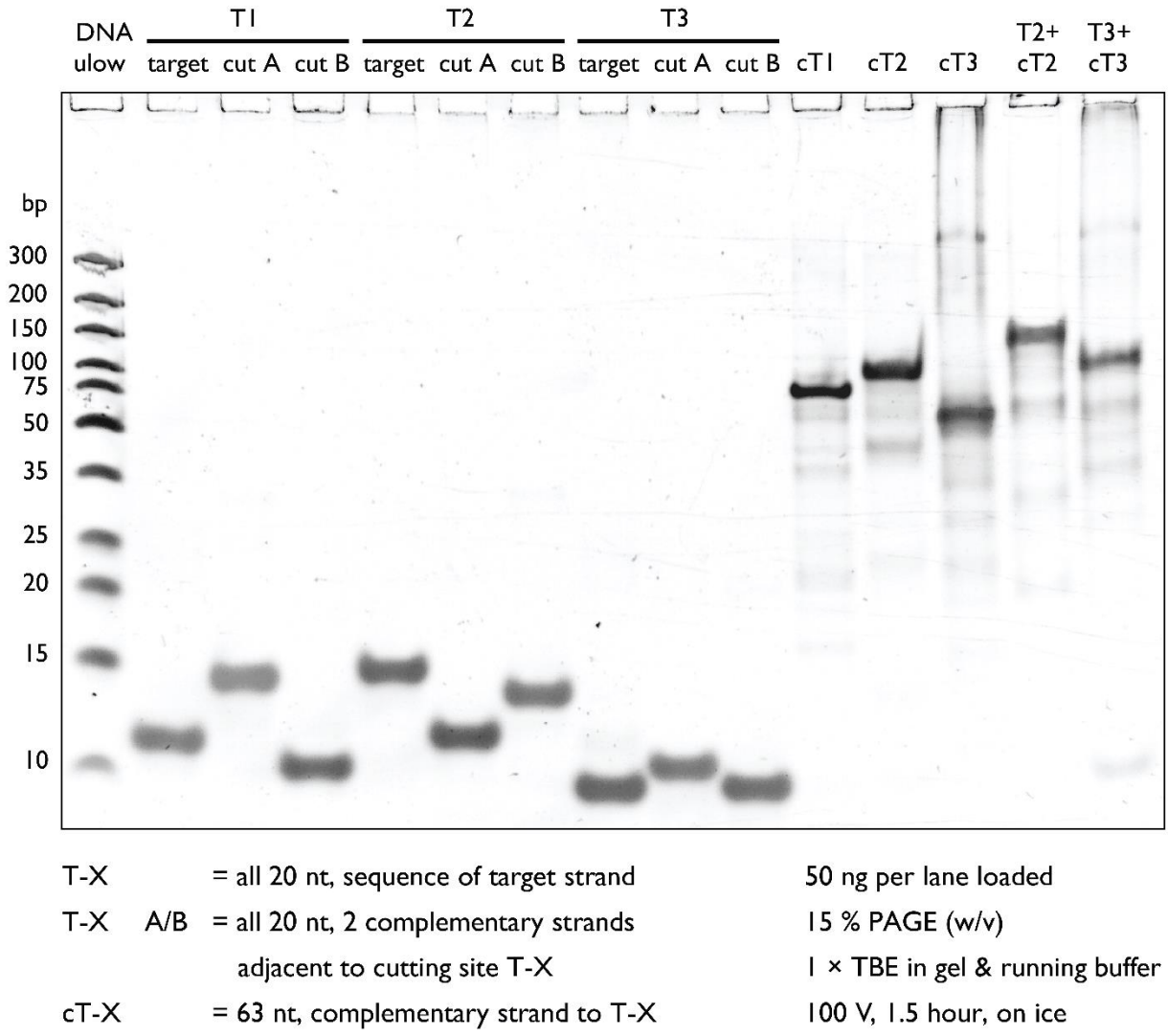

Figure S12. PAGE analysis of oligonucleotides used for MS2 RNase H cutting, target strands, and complementary capture strands. Thermo Scientific™ GeneRuler Ultra Low Range DNA Ladder was used (DNA ulow). Samples were run once.

We performed a control PAGE analysis by treating MS2 RNA with RNase H cutting without guide oligos. Here, we tested if targets have significant binding to enzyme-treated RNA (Figure S13).

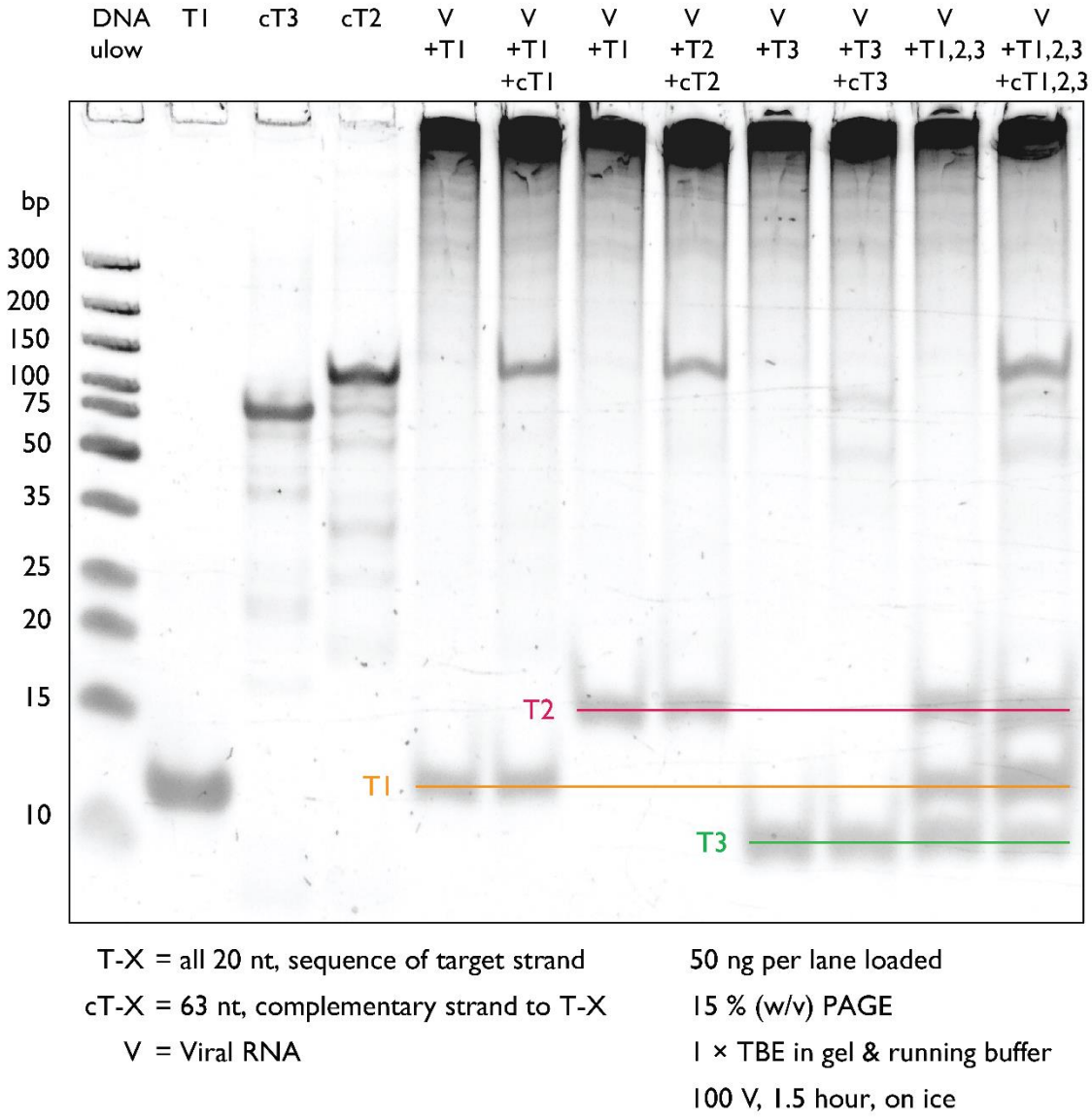

Figure S13. PAGE analysis of oligonucleotide mobility in a background of MS2 RNA treated with RNase H without added guide oligos. Samples were run once.

Previously, we have shown that MS2 RNA is cut in fragments of the desired size with 100 % efficiency. However, the release of target RNAs from cut MS2 RNA cannot be tested using this gel. In Figure S14 we tested if RNA target is free in solution. Once MS2 RNA is cut with one guide oligo, the target is absent (x T1A) and the T1A oligo is the only one visible. If both guide oligos are added for target T1 an additional band is visible on the gel. We wanted to validate that this band is the T1 target. This is performed by mixing cut MS2 with a complementary strand (cT1+30 T; the sequence is listed in Table S23) and observing a shift from the cT1+30 T strand.

In the case of the T2 target, we have not observed any additional band indicating that target M2 is probably bound to its position in MS2 RNA structure, as discussed in the main text.

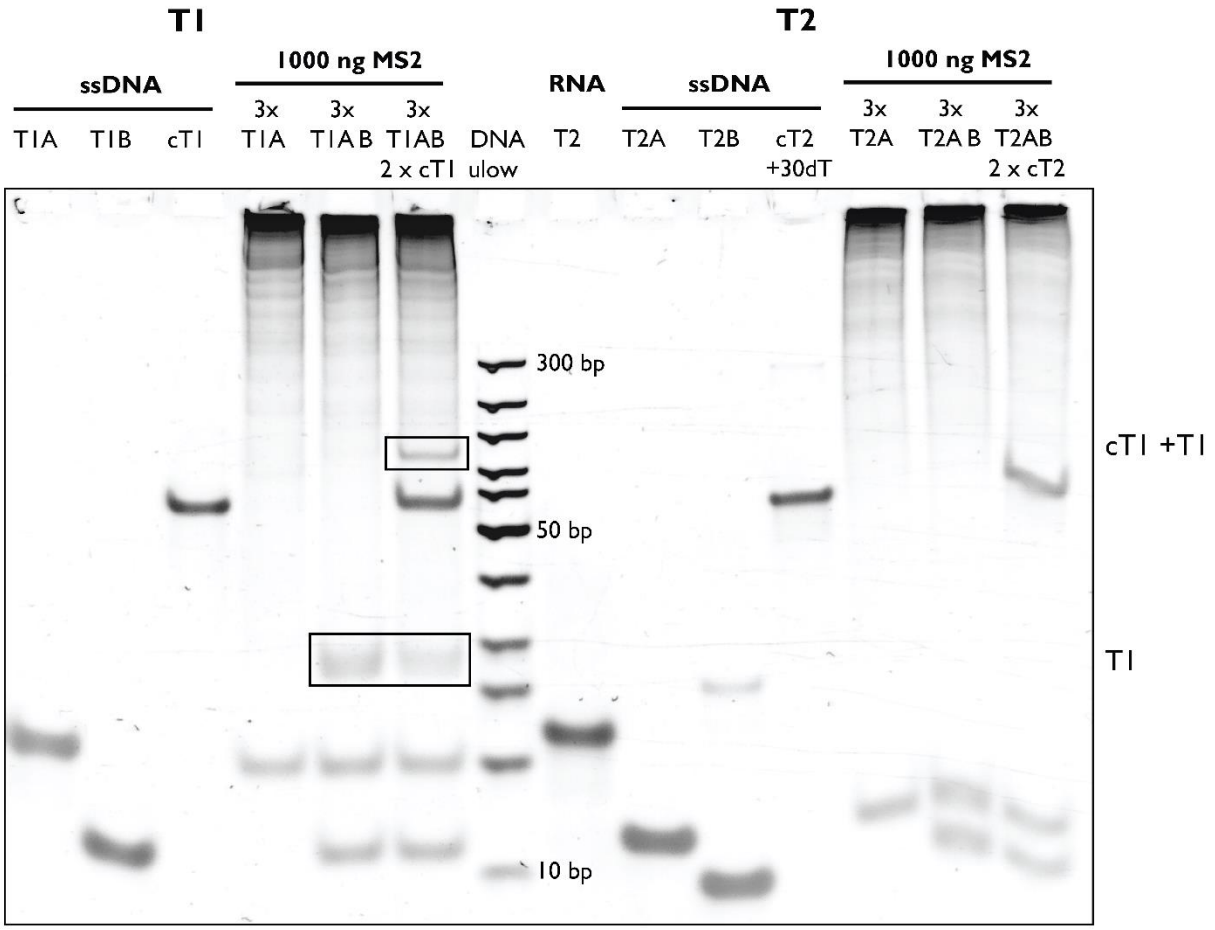

T-X = all 20 nt, sequence of target strand

T-X A/B = all 20 nt, 2 complementary strands adjacent to cutting site T-X

cT-X(+30 dT) = 63 nt, complementary strand to T-X

RNA M2	50 ng
T-X A & B	50 ng
cT-X	30 ng
MS2	1000 ng

15 % (w/v) PAGE

1 × TBE in gel & running buffer

100 V, 1.5 hour, on ice

Figure S14. PAGE analysis of target detection after MS2 RNA is treated with RNase H with respective guide oligos for targets T1 and T2 added. DNA ulow lane corresponds to GeneRuler Uultra Low Range DNA ladder (Thermo Fisher Scientific) with the lowest band being 10 bp and the highest band being 300 bp in length. Samples were run once.

Section S11. DNA nanobait for MS2 RNA target detection

Nanobait for MS2 virus is prepared as previously described in Section S2. Below are listed sequences of capture sites (Table S21), biotin strand (Table S20), and target sequence (Table S19). In Table S22 are listed guide oligos for all targets.

We also show additional nanopore events of nanobait without cut MS2 (Figure S15a), and with cut MS2 RNA added (Figure S15b). The nanobait and peaks resemble those presented in Figure 4b of the manuscript. These single-molecule events are obtained from three separate nanopore measurements.

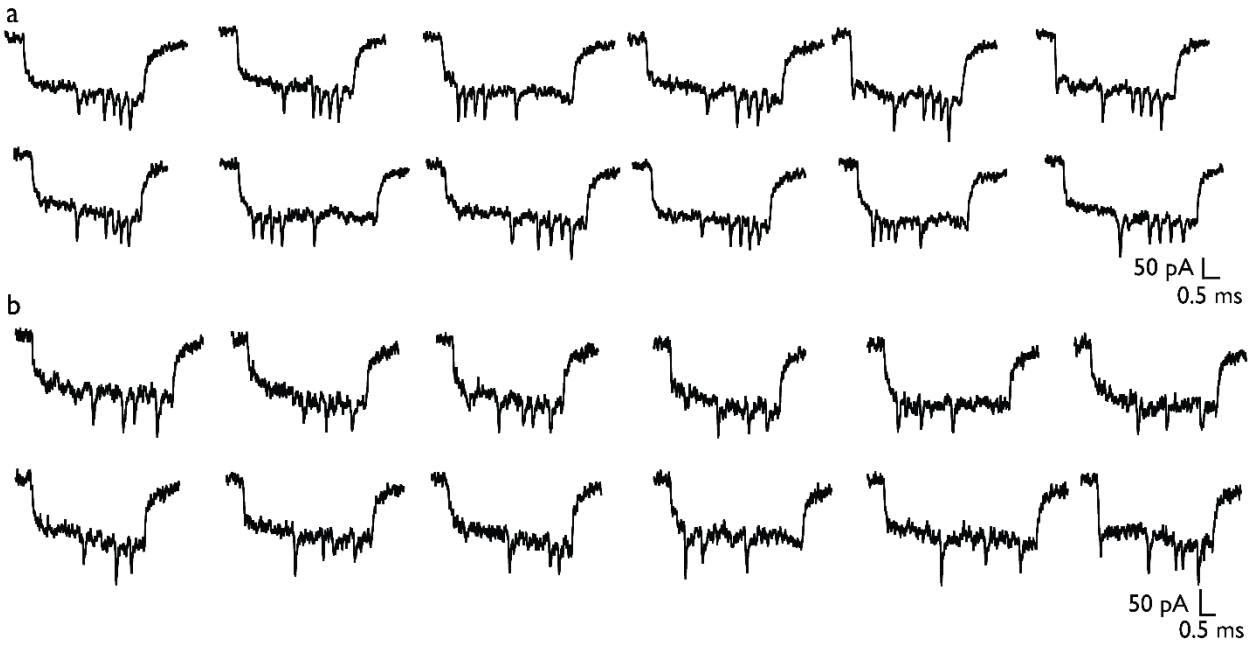

Figure S15. Example events for nanobait with cut MS2 RNA. a) Single-molecule nanobait events indicate that a) all three peaks are present, hence targets are not present, or b) peaks are absent, hence targets are present.

Supplementary Table S18. Presence of peaks at their respective sites for multiple MS2 viral target identification.

Target/Case	Control (no targets)	Standard error	Target present	Standard error
T1	0.08	0.01	0.41	0.01

T2	0.11	0.04	0.25	0.04
T3	0.06	0.03	0.14	0.02

Supplementary Table S19. Target sequences for MS2 target identification.

Strand name	Sequence (5' → 3')
T1	ACCACTAATGAGTGATATCC
T2	TACCTGTAGGTAACATGCTC
T3	TCTGCATCCGATTCCATCTC

Supplementary Table S20. 3' Biotinylated strand sequences for MS2 target identification.

Strand name	Sequence (5' → 3')	Length (nt)
bT1	AATGAGTGATATCC/3'-biotin/	14
bT2	TAGGTAACATGCTC/3'-biotin/	14
bT3	TCCGATTCCATCTC/3'-biotin/	14

Supplementary Table S21. Capture strand sequences for MS2 target identification.

Strand name	Sequence (5' → 3')
cT1_42	TTCGACAACTCGTATTAAATCCTTTGCCCGAACGTTATTTTTT GGATATCACTCATTAGTGGT
cT2_55	GTGAGTGAATAACCTTGCTTCTGTAAATCGTCGCTATT TTTTT GAGCATGTTACCTACAGGTA
cT3_68	AGAATATAAAGTACCGACAAAAGGTAAAGTAATTCTGT TTTTT GAGATGGAATCGGATGCAGA

Supplementary Table S22. Guide oligo sequences for MS2 target identification.

Strand name	Sequence (5’ → 3’)
T1a	AACCAACCGAACTGCAACTC
T1b	AAGCATCTCATATGCACCCT
T2a	GGAGCCAGTCGACAACGAAT
T2b	ACGGGGGCCGTAAGGCCCTC
T3a	CGATAAGTCTATCGTCGCAA
T3b	AACTCCACACCAGGCGATCG

Supplementary Table S23. Complementary strands to MS2 targets with the 30 T-tail used for PAGE gel analysis.

Strand name	Sequence (5’ → 3’)
cM1_30T	TTTTTTTTTTTTTTTTTTTTTTTTTTTTTTGGATATCACTCATTAGTGGT
cM2_30T	TTTTTTTTTTTTTTTTTTTTTTTTTTTTTTGAGCATGTTACCTACAGGTA

Section S12. Detection of SARS-CoV-2 RNA targets from patient samples using DNA nanobait

Nanobait for SARS-CoV-2 virus is prepared as previously described in Section S2. Below are listed sequences of capture sites (Table S26), biotin strand (Table S25), and target sequence (Table S24). In Table S27 are listed guide oligos for all targets.

Supplementary Table S24. Target sequences for SARS-CoV-2 target identification in a patient sample.

Strand name	Sequence (5' → 3')
S1	CATCCTTACTGCGCTTCGAT
S2	CATTGCAACTGAGGGAGCCT
S3	AGACTCAGACTAATTCTCCT

Supplementary Table S25. 3' Biotinylated strand sequences for SARS-CoV-2 target identification in a patient sample.

Strand name	Sequence (5' → 3')	Length (nt)
bS1	TACTGCGCTTCGAT/3'-biotin/	14
bS2	AACTGAGGGAGCCT/3'-biotin/	14
bS3	AGACTAATTCTCCT/3'-biotin/	14

Supplementary Table S26. Capture strand sequences for SARS-CoV-2 target identification in a patient sample.

Strand name	Sequence (5' → 3')
cS1_43	TTCGACAACTCGTATTAAATCCTTTGCCCGAACGTTAT TTTTT ATCGAAGCGCAGTAAGGATG

cS2_55	GTGAGTGAATAACCTTGCTTCTGTAAATCGTCGCTATT TTTTT AGGCTCCCTCAGTTGCAATG
cS3_68	AGAATATAAAGTACCGACAAAAGGTAAAGTAATTCTGT TTTTT AGGAGAATTAGTCTGAGTCT

Supplementary Table S27. Guide DNA oligo sequences for SARS-CoV-2 target identification in patient samples.

Strand name	**Sequence (5' → 3')**
S1a	GCTAGTGTAACTAGCAAGAA
S1b	ATTGCAGCAGTACGCACACA
S2a	CGTTCTCCATTCTGGTTACT
S2b	GTGATCTTTTGGTGTATTCA
S3a	GATAACTAGCGCATATACCT
S3b	GCTACACTACGTGCCCGCCG

Section S13. Detection of SARS-CoV-2 RNA targets from patient samples using DNA nanobait and DNA flower as a label

The nanobait synthesis follows the previously presented protocol including RNase H cutting and the SDR. As shown in Figure S16, to construct the reference structures on the nanobait, staples 26-32 and 96-102 were substituted by the relevant dumbbell sequences (Table S29). To link the DNA flowers onto the nanobait, staple 43 was substituted by strand P43 and C43 (C43 was added during preparation of 7WJa, so only P43 was added), staple 57 was substituted by strand C57 and P57, and staple 68 was substituted by strand cS3-68. The staples were mixed, and then the linear M13 scaffold was added into the solution (20 nM M13 scaffold, 60 nM staples, 120 nM dumbbell strands, and 120 nM P43, C57, P57, cS3-68). The mixture was heated to 70 °C followed by a linear cooling ramp to 25 °C over 50 minutes. 1 μL of 4 μM 7WJa, 7WJb, and 7WJc (DNA flowers) were added into the 40 μL nanobait solution and incubated at room temperature for 2 h. Finally, the resulted solution was diluted with a washing buffer (10 mM Tris-HCl, 0.5 mM $MgCl_2$, pH 8.0) to 500 μL and centrifuged at 6000 × g for 10 min with an Amicon Ultra 100 kDa filter to remove the excess DNA strands and DNA flowers (repeated 3 times). About 35 μL of nanobait solution was obtained and quantified with a NanoDrop 2000 spectrophotometer.

The flower nanobait for the COVID-19 patient sample was diluted to 250 pM. 3.8 μL of a patient sample (positive or negative samples were processed by the programmable RNase H cutting step) was mixed with 0.2 μL of 250 pM nanobait, 0.5 μL of 100 mM $MgCl_2$, and 0.5 μL of 1 M NaCl. The mixture (5 μL) was incubated at room temperature for 10 min and then diluted by 5 μL of 8 M LiCl and 20 μL of 4 M LiCl (in 1 × TE, pH 9.0) proceeding the nanopore measurement.

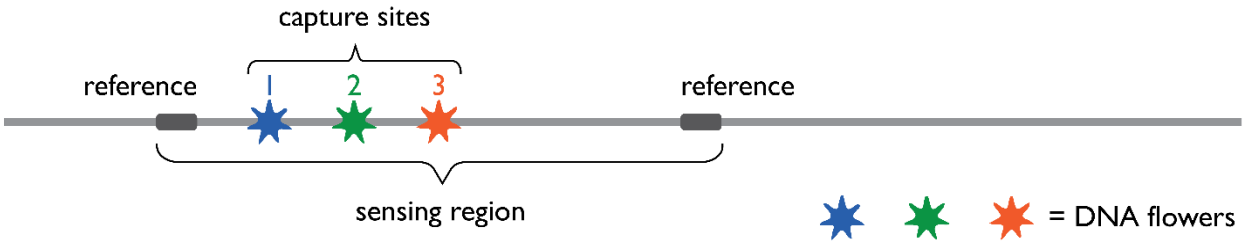

Figure S16. Design of nanobait with the DNA flower labels for testing COVID-19 patient sample. Each of the references is represented by eleven closely spaced DNA dumbbells.

Oligonucleotide sequences for DNA flower-based detection with nanobait are listed in Table S28. Example events for negative and positive SARS-CoV-2 patient samples obtained using DNA flowers are shown in Figure S17a and Figure S17b, respectively.

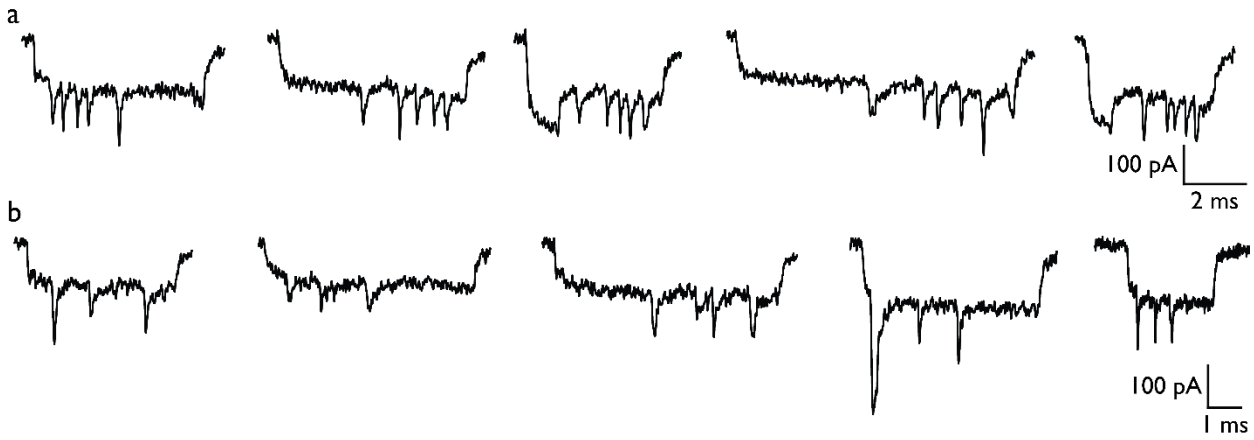

Figure S17. Example events of nanobait with DNA flower labels incubated with negative and positive SARS-CoV-2 patient samples (a and b, respectively).

Supplementary Table S28. Capture strand sequences for SARS-CoV-2 target identification in a patient sample using DNA flower as a label.

Strand name	Replaced oligo #	Sequence (5' → 3')
cFS1_43	43	TAATTTTAAAAGTTTGAGTA TT ATCGAAGCGCAGTA AGGATG
43+	43	ACATTATCATTTTGCGGA
cFS2_57	57	AGCTTAGATTAAGACGCTGA TT AGGCTCCCTCAGTT GCAATG
57+	57	GAAGAGTCAATAGTGAAT
cFS3_68	68	AGAATATAAAGTACCGACAAAAGGTAAAGTAATTCTGT TTTTT AGGAGAATTAGTCT GAGTCT

Supplementary Table S29. List of oligonucleotides that were replaced from Table S2 to assemble reference structures for nanobait with DNA flower. DNA dumbbell forming sequence is indicated in red.

Strand name	Sequence (5' → 3')	Length (nt)	Replaced oligo #
*REF 1.1	CTGAAAGCGTAAGAATACGTGGCACAGACAATATTTTTGAATGGCT	46	
*REF 1.2	ACATCACTTGTCCTCTTTTGAGGAACAAGTTTTCTTGTCCTGAGTAGA	48	
*REF 1.3	AGAACTCAAATCCTCTTTTGAGGAACAAGTTTTCTTGTCTATCGGCCT	48	
*REF 1.4	TGCTGGTAATTCCTCTTTTGAGGAACAAGTTTTCTTGTATCCAGAACA	48	
*REF 1.5	ATATTACCGCTCCTCTTTTGAGGAACAAGTTTTCTTGTCAGCCATTGC	48	
*REF 1.6	AACAGGAAAATCCTCTTTTGAGGAACAAGTTTTCTTGTACGCTCATGG	48	26-32
*REF 1.7	AAATACCTACTCCTCTTTTGAGGAACAAGTTTTCTTGTATTTTGACGC	48	
*REF 1.8	TCAATCGTCTTCCTCTTTTGAGGAACAAGTTTTCTTGTGAAATGGATT	48	
*REF 1.9	ATTTACATTGTCCTCTTTTGAGGAACAAGTTTTCTTGTGCAGATTCAC	48	
*REF 1.10	CAGTCACACGTCCTCTTTTGAGGAACAAGTTTTCTTGTACCAGTAATA	48	
*REF 1.11	AAAGGGACATTCCTCTTTTGAGGAACAAGTTTTCTTGTTCTGGCCAAC	48	
*REF 1.12	AGAGATAGAATCCTCTTTTGAGGAACAAGTTTTCTTGTCCCTTCTGAC	48	
*REF 2.1	CTTGAGCCATTCCTCTTTTGAGGAACAAGTTTTCTTGTTTGGGAATTA	48	
*REF 2.2	GAGCCAGCAATCCTCTTTTGAGGAACAAGTTTTCTTGTAATCACCAGT	20	
*REF 2.3	AGCACCATTATCCTCTTTTGAGGAACAAGTTTTCTTGTCCATTAGCAA	48	96-102
*REF 2.4	GGCCGGAAACTCCTCTTTTGAGGAACAAGTTTTCTTGTGTCACCAATG	48	
*REF 2.5	AAACCATCGATCCTCTTTTGAGGAACAAGTTTTCTTGTTAGCAGCACC	48	
*REF 2.6	GTAATCAGTATCCTCTTTTGAGGAACAAGTTTTCTTGTGCGACAGAAT	48	

*REF 2.7	CAAGTTTGCCTCCTCTTTTGAGGAACAAGTTTTCTTGTTTTAGCGTCA	48
*REF 2.8	GACTGTAGCGTCCTCTTTTGAGGAACAAGTTTTCTTGTCGTTTTCATC	48
*REF 2.9	GGCATTTTCGTCCTCTTTTGAGGAACAAGTTTTCTTGTGTCATAGCCC	48
*REF 2.10	CCTTATTAGCTCCTCTTTTGAGGAACAAGTTTTCTTGTGTTTGCCATC	48
*REF 2.11	TTTTCATAATTCCTCTTTTGAGGAACAAGTTTTCTTGTCAAAATCACC	48
*REF 2.12	GGAACCAGAGCCACCACCGGAACCGCCTCCCTCAGAGCCGCCACCC	46

Section S14. Nanopore data analysis

Data analysis of nanopore current traces is performed as previously described [1,4,16]. The data analysis workflow is shown in Figure S18. Firstly, in a raw ionic current trace, our home-built LabView script identifies events by specifying the event duration range and the current threshold. In the next step, nanobait events are separated from isolated events with too small and too large event charge deficit (ECD). Nanobaits can translocate through the nanopore as unfolded or folded (Figure S18). Downward peaks were identified as described previously[1]. The key advantage of nanobait is its pre-determined design relying on the identification of unique current signatures[1,17]. A specific current drop threshold correlating to approximately double the baseline noise was used to identify peaks. Firstly, the reference peaks are identified and positioned. Next, the presence of the peaks corresponding to our sensing sites was identified and an appropriate color was assigned. Lastly, we determine present peaks and calculate displacement efficiency for each site.

Nanopore events can be analyzed with the convolutional neural network QuipuNet following the procedure outlined in Figure S18. Its event detection is much faster, with the rate of 1600 events/s, making it appropriate for instantaneous, real-time data analysis[16] that is not achievable with the other detection methods[18–20].

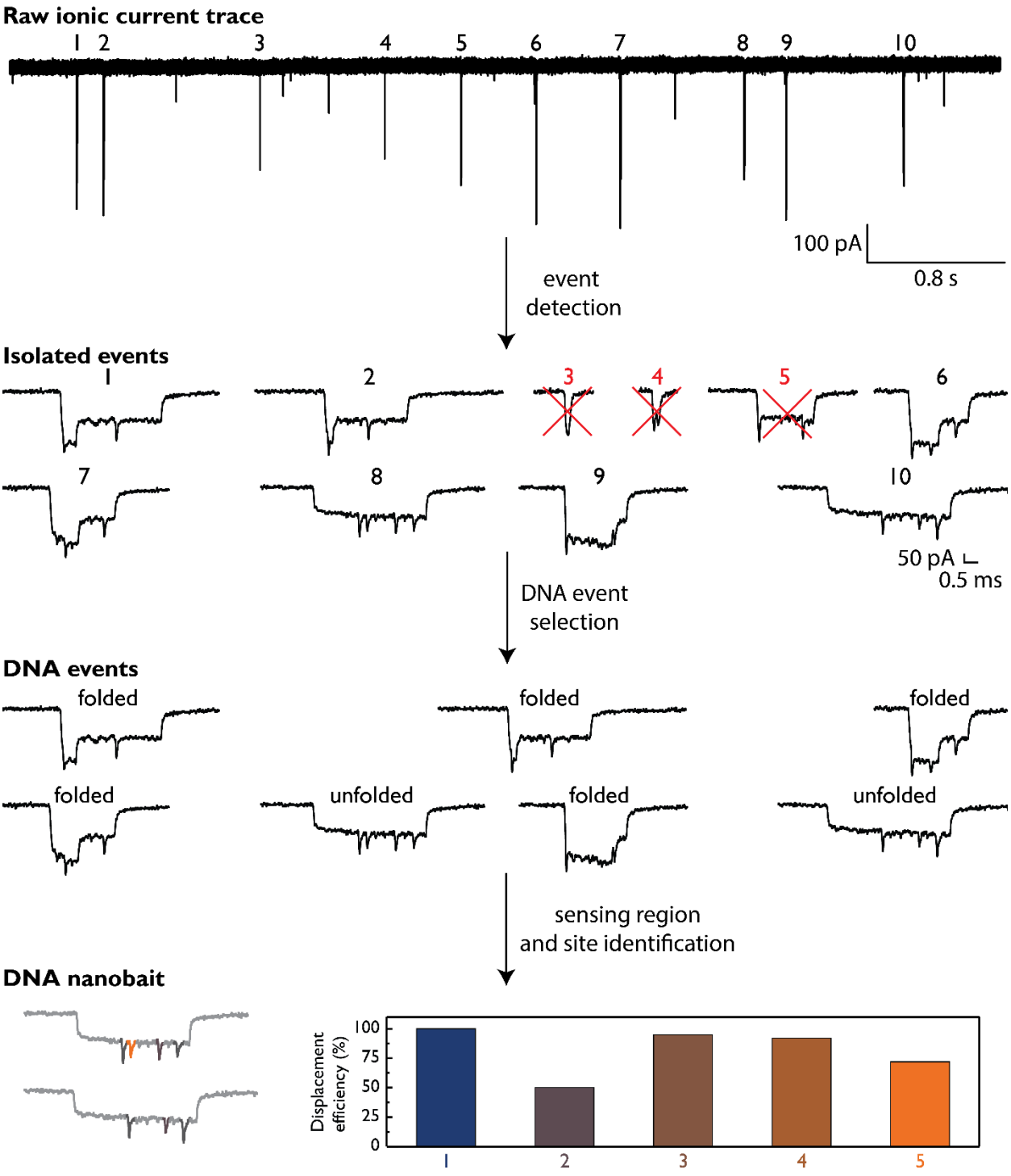

Figure S18. Nanopore data analysis workflow. The data analysis starts by searching for single-molecule events from the raw nanopore ionic current traces. Event's duration, current drop, and event charge deficit (ECD i.e. event's surface area) are parameters that further separate nanobait events from DNA events. DNA events in nanopore measurements can include bent or folded

events and linear or unfolded events. The next analysis step includes identifying the sensing region (marked by two references) and the absence of the peaks at their respective sites. In the last step, we calculate the mean and errors from multiple single-molecule events (from multiple nanopores), that are subtracted to the control measurement and presented as the displacement efficiency in the bar chart.

Section S15. Nanopore statistics

Nanopore measurements are listed in Table S30 with characteristics of both nanopores used and sample presented. In all measurements, the first fifty unfolded nanobaits were used for the displacement efficiency calculations unless otherwise specified. All measurements were obtained under an applied field of 600 mV and the respective ionic current value is indicated in Table S30. Only nanopores with the linear current-voltage curve and the noise root mean square (RMS) of < 7 pA were used for nanopore measurements.

Supplementary Table S30. Nanopore measurement details for all experiments presented in this study.

Nanopore measurement	DNA nanobait type / sample name	Current at 600 mV (nA)	Target present	RNase H cutting	Human total RNA	Patient sample	Excess of targets (times)	Incubation time (min)
1	Blank	10	/	/	/	/	10	10
2	Blank	11	/	/	/	/	10	10
3	Blank	14.5	/	/	/	/	10	10
4	Blank	14	/	/	/	/	10	10
5	Blank	11	/	/	/	/	10	10
6	Blank	7	/	/	/	/	10	10
7	Blank	12	/	/	/	/	10	10
8	Blank	8	/	/	/	/	10	10
9	H1-H5	12.4	five targets	/	/	/	10	10
10	H1-H5	9.8	five targets	/	/	/	10	10
11	H1-H5	12.15	five targets	/	/	/	10	10
12	H1-H5	12.3	five targets	/	/	/	10	10
13	total RNA + Nanobait	9.5	/	/	yes	/	10	10
14	total RNA + Nanobait	10.2	/	/	yes	/	10	10
15	total RNA + Nanobait	10	/	/	yes	/	10	10
16	total RNA + Nanobait+targets	9.4	five targets	/	yes	/	10	10
17	total RNA + Nanobait+targets	9.25	five targets	/	yes	/	10	10
18	total RNA + Nanobait+targets	10.5	five targets	/	yes	/	10	10

19	Nanobait + negative covid sample a53	9	/	/	/	negative	NA	10
20	Nanobait + negative covid sample a53	9	/	/	/	negative	NA	10
21	Nanobait + negative covid sample a53	10.6	/	/	/	negative	NA	10
22	Nanobait + negative covid sample a55	10.2	/	/	/	negative	NA	10
23	Nanobait + negative covid sample a55	11	/	/	/	negative	NA	10
24	Nanobait + negative covid sample a55	8.72	/	/	/	negative	NA	10
25	Nanobait + negative covid sample+targets	10.5	/	/	/	negative	NA	10
26	Nanobait + negative covid sample+targets	10.25	/	/	/	negative	NA	10
27	Nanobait + negative covid sample+targets	11	/	/	/	negative	NA	10
28	Nanobait + negative covid sample+RNaseH cutting	10.2	/	yes	/	negative	NA	10
29	Nanobait + negative covid sample+RNaseH cutting	9.8	/	yes	/	negative	NA	10
30	kinetics 1 min DNA	9.8	all targets	/	/	/	10	1
31	kinetics 2.5 min DNA	10.9	all targets	/	/	/	10	2.5
32	kinetics 5 min DNA	11.2	all targets	/	/	/	10	5
33	kinetics 10 min DNA	10	all targets	/	/	/	10	10
34	kinetics 1 min RNA	12	all targets	/	/	/	10	1
35	kinetics 2.5 min RNA	12.4	all targets	/	/	/	10	2.5
36	kinetics 5 min RNA	12.2	all targets	/	/	/	10	5
37	kinetics 10 min RNA	10	all targets	/	/	/	10	10
38	Nanobait for MS2 blank	12	/	/	/	/	10	10
39	Nanobait for MS2 blank	11	/	/	/	/	10	10
40	Nanobait for MS2 blank	11	/	/	/	/	10	10
41	Nanobait for MS2 blank+targets	11.58	all targets	/	/	/	10	10
42	Nanobait for MS2 blank+targets	10.8	all targets	/	/	/	10	10

43	Nanobait for MS2 blank+RNaseH cutting	10	/	yes	/	/	10	10
44	Nanobait for MS2 blank+RNaseH cutting	12.5	/	yes	/	/	10	10
45	Nanobait for MS2 blank+RNaseH cutting	13.1	/	yes	/	/	10	10
46	Nanobait for a patient covid sample	11	/	/	/	/	10	10
47	Nanobait for a patient covid sample	10.7	/	/	/	/	10	10
48	Nanobait for patient covid sample+negative sample	9.9	/	yes	/	negative	NA	10
49	Nanobait for patient covid sample+positive sample	9.8	/	yes	/	positive	NA	10
50	Nanobait for patient covid sample+positive sample	10.7	/	yes	/	positive	NA	10
51	Nanobait for patient covid sample+positive sample	10.4	/	yes	/	positive	NA	10
52	Nanobait for patient covid sample with DNA flower	6.98	/	/	/	/	10	10
53	Nanobait for patient covid sample with DNA flower+negative sample	11.4	/	yes	/	negative	NA	10
54	Nanobait for patient covid sample with DNA flower+negative sample	11.18	/	yes	/	negative	NA	10
55	Nanobait for patient covid sample with DNA flower	11.44	/	yes	/	positive	NA	10
56	Nanobait for patient covid sample with DNA flower	9.89	/	yes	/	positive	NA	10
57	Nanobait for patient covid sample with DNA flower	10.1	/	yes	/	positive	NA	10
58	Nanobait for multiple viruses blank	9	/	/	/	/	10	10

59	Nanobait for multiple viruses blank	7.5	/	/	/	/	10	10
60	Nanobait for multiple viruses blank	8.5	/	/	/	/	10	10
61	Nanobait for multiple viruses blank+all targets	8.8	all targets	/	/	/	10	10
62	Nanobait for multiple viruses blank+all targets	8	all targets	/	/	/	10	10
63	Nanobait for multiple viruses blank+all targets	11	all targets	/	/	/	10	10
64	Nanobait for multiple viruses blank+SARS-CoV-2 target	8.6	SARS-CoV-2	/	/	/	10	10
65	Nanobait for multiple viruses blank+SARS-CoV-2 target	10.15	SARS-CoV-2	/	/	/	10	10
66	Nanobait for multiple viruses blank+SARS-CoV-2 target	11.4	SARS-CoV-2	/	/	/	10	10
67	Nanobait for multiple viruses blank+Influenza target	8.99	Influenza	/	/	/	10	10
68	Nanobait for multiple viruses blank+Influenza target	9.42	Influenza	/	/	/	10	10
69	Nanobait for multiple viruses blank+Influenza target	14.8	Influenza	/	/	/	10	10
70	Nanobait for multiple viruses blank+RSV target	9.54	RSV	/	/	/	10	10
71	Nanobait for multiple viruses blank+RSV target	15.15	RSV	/	/	/	10	10
72	Nanobait for multiple viruses blank+RSV target	9.3	RSV	/	/	/	10	10
73	Nanobait for multiple viruses blank+Parainfluenza target	9.6	Parainfluenza	/	/	/	10	10
74	Nanobait for multiple viruses	9.67	Parainfluenza	/	/	/	10	10

	blank+Parainfluenza target							
75	Nanobait for multiple viruses blank+Parainfluenza target	15.2	Parainfluenza	/	/	/	10	10
76	Nanobait for multiple viruses blank+Rhinoviruses target	8.9	Rhinoviruses	/	/	/	10	10
77	Nanobait for multiple viruses blank+Rhinoviruses target	15.5	Rhinoviruses	/	/	/	10	10
78	Nanobait for multiple viruses blank+Rhinoviruses target	9.74	Rhinoviruses	/	/	/	10	10
79	Nanobait for variants blank	9.01	/	/	/	/	10	10
80	Nanobait for variants blank	9.7	/	/	/	/	10	10
81	Nanobait for variants blank	8.52	/	/	/	/	10	10
82	Nanobait for variants blank + WT targets	8.5	all targets	/	/	/	10	10
83	Nanobait for variants blank + WT targets	8.5	all targets	/	/	/	10	10
84	Nanobait for variants blank + WT targets	7.8	all targets	/	/	/	10	10
85	Nanobait for variants blank + variant targets	8.8	all targets	/	/	/	10	10
86	Nanobait for variants blank + variant targets	9.03	all targets	/	/	/	10	10
87	Nanobait for variants blank + variant targets	9	all targets	/	/	/	10	10
88	Nanobait for variants+SARS-CoV-2 reference variant target	11.5	SARS-CoV-2 reference	/	/	/	10	10
89	Nanobait for variants+ SARS-CoV-2 reference variant target	10.5	SARS-CoV-2 reference	/	/	/	10	10
90	Nanobait for variants+ SARS-CoV-2 reference variant target	9.7	SARS-CoV-2 reference	/	/	/	10	10

91	Nanobait for variants+Delta variant target	10	Delta	/	/	/	10	10
92	Nanobait for variants+Delta variant target	10	Delta	/	/	/	10	10
93	Nanobait for variants+Delta variant target	12	Delta	/	/	/	10	10
94	Nanobait for variants+ B.1 variant target	10.1	B.1	/	/	/	10	10
95	Nanobait for variants+ B.1 variant target	13.75	B.1	/	/	/	10	10
96	Nanobait for variants+ B.1 variant target	12.8	B.1	/	/	/	10	10
97	Nanobait for variants+Alpha variant target	10.68	Alpha	/	/	/	10	10
98	Nanobait for variants+Alpha variant target	8.3	Alpha	/	/	/	10	10
99	Nanobait for variants+Alpha variant target	11.3	Alpha	/	/	/	10	10
100	Nanobait for variants+Beta variant target	9.5	Beta	/	/	/	10	10
101	Nanobait for variants+Beta variant target	9.7	Beta	/	/	/	10	10
102	Nanobait for variants+Beta variant target	14.1	Beta	/	/	/	10	10
103	Nanobait for patient covid sample+negative sample	11	/	yes	/	negative	NA	10
104	Nanobait for patient covid sample+negative sample	12	/	yes	/	negative	NA	10
105	Nanobait for patient covid sample+negative sample	9.7	/	yes	/	negative	NA	10
106	Nanobait for patient covid sample+negative sample	11	/	yes	/	negative	NA	10
107	Nanobait for patient covid	11.5	/	yes	/	negative	NA	10

	sample+negative sample							
108	Nanobait for patient covid sample+negative sample	10	/	yes	/	negative	NA	10
109	Nanobait for patient covid sample+negative sample	11.1	/	yes	/	negative	NA	10
110	Nanobait for patient covid sample+negative sample	11.3	/	yes	/	negative	NA	10
111	Nanobait for patient covid sample+negative sample	11.8	/	yes	/	negative	NA	10
112	Nanobait for SARS-CoV-2 RNA N501	7	/	/	/	/	10	10
113	Nanobait for SARS-CoV-2 RNA N501+wild-type	8.36	WT	yes	/	/	10	10
114	Nanobait for SARS-CoV-2 RNA N501+wild-type	7.6	WT	yes	/	/	10	10
115	Nanobait for SARS-CoV-2 RNA N501+wild-type	5.6	WT	yes	/	/	10	10
116	Nanobait for SARS-CoV-2 RNA N501+N501S	12.78	N501S	yes	/	/	10	10
117	Nanobait for SARS-CoV-2 RNA N501+ N501S	8.7	N501S	yes	/	/	10	10
118	Nanobait for SARS-CoV-2 RNA N501+ N501S	9	N501S	yes	/	/	10	10
119	Nanobait for SARS-CoV-2 RNA N501+N501T	12.6	N501T	yes	/	/	10	10
120	Nanobait for SARS-CoV-2 RNA N501+ N501T	8.2	N501T	yes	/	/	10	10
121	Nanobait for SARS-CoV-2 RNA N501+ N501T	14	N501T	yes	/	/	10	10

Section S16. Sensitivity curve

We prepared serial dilutions of nanobait with SARS-CoV-2 N501 WT cut RNA (Figure S19a; details in Section S8). Any contact surfaces were passivated with a 20 bp DNA (5 nM; 5'-GACCACTACAGTTGTAATCC-3' IDT) prior to contact with the diluted samples to prevent surface binding. The sensitivity curve was shown from fM to nM range of nanobait concentrations.

Nanobait was mixed with SARS-CoV-2 RNA targets (20 nt, H2 and H5 sequences in Supplementary Table S15) in various ratios of RNA for 10 min and by keeping nanobait concentration constant (Figure S19b).

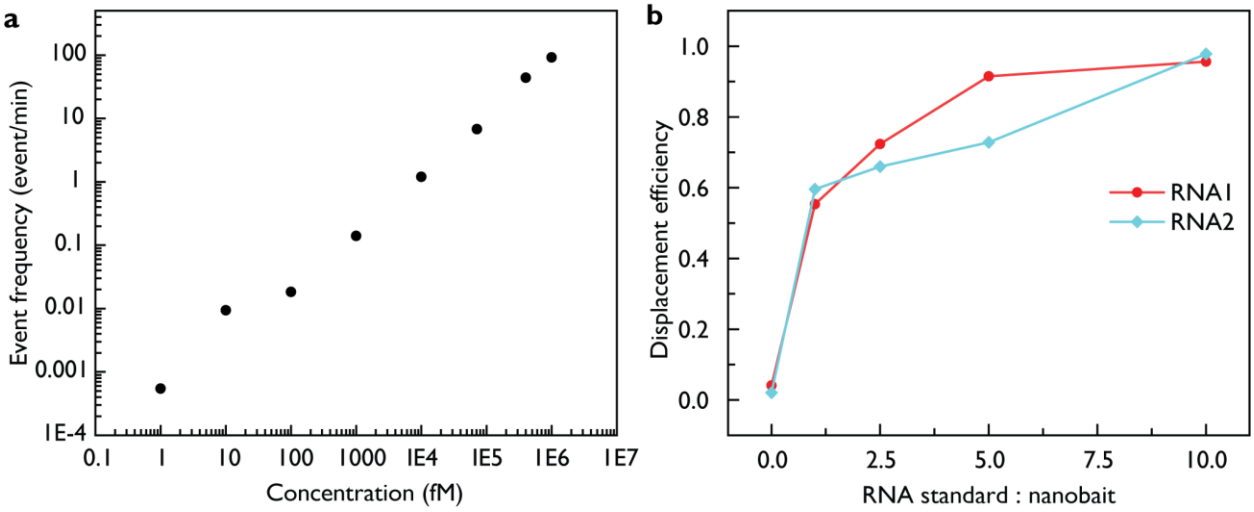

Figure S19. Sensitivity curve of nanobait-nanopore system. **a)** Nanobait detection with SARS-CoV-2 N501 wild-type target as described in Section S8. Were detected in the range from femtomolar (fM) to nanomolar (nM) concentrations. Event frequency was plotted as a function of log of nanobait concentration in fM versus log of event frequency in events per min. **b)** Nanobait displacement efficiency with variable SARS-CoV-2 RNA concentrations. Nanobait concentration was constant at 500 pM and viral RNAs (RNA1 and RNA2 correspond to H2 and H4, respectively; 20 nt) were varied from 1:1 ratio to 1:10 excess to nanobait to test dynamic range of nanobait.

REFERENCES

1. Bell, N. A. W. & Keyser, U. F. Digitally encoded DNA nanostructures for multiplexed, single-molecule protein sensing with nanopores. *Nature Nanotechnology* **11**, 645–651 (2016).

2. Stahl, E., Martin, T. G., Praetorius, F. & Dietz, H. Facile and Scalable Preparation of Pure and Dense DNA Origami Solutions. *Angewandte Chemie International Edition* **53**, 12735–12740 (2014).

3. Ohmann, A. *et al.* Controlling aggregation of cholesterol-modified DNA nanostructures. *Nucleic Acids Res* **47**, 11441–11451 (2019).

4. Bošković, F., Ohmann, A., Keyser, U. F. & Chen, K. DNA Structural Barcode Copying and Random Access. *Small Structures* **2**, 2000144 (2021).

5. Chen, K., Zhu, J., Bošković, F. & Keyser, U. F. Nanopore-based dna hard drives for rewritable and secure data storage. *Nano Letters* **20**, 3754–3760 (2020).

6. Fairhead, M., Krndija, D., Lowe, E. D. & Howarth, M. Plug-and-Play Pairing via Defined Divalent Streptavidins. *Journal of Molecular Biology* **426**, 199–214 (2014).

7. Zhu, J., Ermann, N., Chen, K. & Keyser, U. F. Image Encoding Using Multi-Level DNA Barcodes with Nanopore Readout. *Small* **17**, 2100711 (2021).

8. Schindelin, J. *et al.* Fiji: An open-source platform for biological-image analysis. *Nature Methods* **9**, 676–682 (2012).

9. Lu, X. *et al.* Real-time reverse transcription-PCR assay for comprehensive detection of human rhinoviruses. *Journal of Clinical Microbiology* **46**, 533–539 (2008).

10. Templeton, K. E., Scheltinga, S. A., Beersma, M. F. C., Kroes, A. C. M. & Claas, E. C. J. Rapid and Sensitive Method Using Multiplex Real-Time PCR for Diagnosis of Infections by Influenza A and Influenza B Viruses, Respiratory Syncytial Virus, and Parainfluenza Viruses 1, 2, 3, and 4. *Journal of Clinical Microbiology* **42**, 1564–1569 (2004).

11. Wu, F. *et al.* A new coronavirus associated with human respiratory disease in China. *Nature* **579**, 265–269 (2020).

12. https://www.who.int/influenza/gisrs_laboratory/WHO_information_for_the_molecular_detection_of_influenza_viruses_20171023_Final.pdf.

13. Shirato, K. *et al.* Diagnosis of human respiratory syncytial virus infection using reverse transcription loop-mediated isothermal amplification. *Journal of Virological Methods* **139**, 78–84 (2007).

14. Konings, F. *et al.* SARS-CoV-2 Variants of Interest and Concern naming scheme conducive for global discourse. *Nature Microbiology* **6**, 821–823 (2021).

15. Rambaut, A. *et al.* A dynamic nomenclature proposal for SARS-CoV-2 lineages to assist genomic epidemiology. *Nature Microbiology* **5**, 1403–1407 (2020).

16. Misiunas, K., Ermann, N. & Keyser, U. F. QuipuNet: Convolutional Neural Network for Single-Molecule Nanopore Sensing. *Nano Letters* **18**, 4040–4045 (2018).

17. Bošković, F. & Keyser, U. F. Nanopore microscope identifies RNA isoforms with structural colors. *bioRxiv* 2021.10.16.464631 (2021) doi:10.1101/2021.10.16.464631.

18. Europe, W. H. Organization. R. O. for. Methods for the detection and identification of SARS-CoV-2 variants. *World Health Organization. Regional Office for Europe* (2021) doi:10.1002/9781119650034.ch16.

19. Caliendo, A. M. Multiplex PCR and emerging technologies for the detection of respiratory pathogens. *Clinical Infectious Diseases* **52**, 326–330 (2011).

20. Zhou, L. *et al.* Programmable low-cost DNA-based platform for viral RNA detection. *Science Advances* **6**, eabc6246 (2020).